

Identifiability of the Simplex Volume Minimization Criterion for Blind Hyperspectral Unmixing: The No Pure-Pixel Case

Chia-Hsiang Lin[†], Wing-Kin Ma[‡], Wei-Chiang Li^{*}, Chong-Yung Chi[§], and ArulMurugan Ambikapathi[◇]

Abstract— In blind hyperspectral unmixing (HU), the pure-pixel assumption is well-known to be powerful in enabling simple and effective blind HU solutions. However, the pure-pixel assumption is not always satisfied in an exact sense, especially for scenarios where pixels are heavily mixed. In the no pure-pixel case, a good blind HU approach to consider is the minimum volume enclosing simplex (MVES). Empirical experience has suggested that MVES algorithms can perform well without pure pixels, although it was not totally clear why this is true from a theoretical viewpoint. This paper aims to address the latter issue. We develop an analysis framework wherein the perfect endmember identifiability of MVES is studied under the noiseless case. We prove that MVES is indeed robust against lack of pure pixels, as long as the pixels do not get too heavily mixed and too asymmetrically spread. The theoretical results are supported by numerical simulation results.

Index Terms— Hyperspectral unmixing, minimum volume enclosing simplex, identifiability, convex geometry, pixel purity measure

I. INTRODUCTION

Signal, image and data processing for hyperspectral imaging has recently received enormous attention in remote sensing [1], [2], having numerous applications such as environmental monitoring, land mapping and classification, and object detection. Such developments are made possible by exploiting the unique features of hyperspectral images, most notably, their high spectral resolutions. In this scope, blind hyperspectral

unmixing (HU) is one of the topics that has aroused much interest not only from remote sensing [3], but also from other communities recently [4]–[7]. Simply speaking, the problem of blind HU is to solve a problem reminiscent of blind source separation in signal processing, and the desired outcome is to unambiguously separate the endmember spectral signatures and their corresponding abundance maps from the observed hyperspectral scene, with no or little prior information of the mixing system. Being given little information to solve the problem, blind HU is a challenging—but also fundamentally intriguing—problem with many possibilities. Readers are referred to some recent articles for overview of blind HU [3], [4], and here we shall not review the numerous possible ways to perform blind HU. The focus, as well as the contribution, of this paper lie in addressing a fundamental question arising from one important blind HU approach, namely, the minimum volume enclosing simplex (MVES) approach.

Also called simplex volume minimization or minimum volume simplex analysis (MVSA) [8], the MVES approach adopts a criterion that exploits the convex geometry structures of the observed hyperspectral data to blindly identify the endmember spectral signatures. In the HU context the MVES concepts were first advocated by Craig back in the 1990's [9], although it is interesting to note an earlier work in mathematical geology [10] which also described the MVES intuitions; see also [4] for a historical note of convex geometry, and the references therein. In particular, Craig's work proposes the use of simplex volume as a metric for blind HU, which is later used in some other blind HU approaches such as simplex volume maximization [11]–[13] and non-negative matrix factorization [14]. The MVES criterion is to minimize the volume of a simplex, subject to constraints that the simplex encloses all hyperspectral data points. This amounts to a nonconvex optimization problem, and unlike the simplex volume maximization approach we do not seem to have a simple (closed-form) scheme for tackling the MVES problem. However, recent advances in optimization have enabled us to handle MVES implementations efficiently. The works in [8] and [6] independently developed practical MVES optimization algorithms based on iterative linear approximation and alternating linear programming, respectively. The GPU-implementation of the former is also considered very recently [15]. In addition, some recent MVES algorithm designs deal with noise and outlier sensitivity issues by robust formulations, such as the soft constraint formulation in SISAL [16] and the chance-constrained formulation in [17]; the pixel elimination method

Part of this paper was presented at the 38th IEEE ICASSP, Vancouver, Canada, May 26-31, 2013. This work was supported in part by the National Science Council (R.O.C.) under Grant NSC 102-2221-E-007-035-MY2, in part by NTHU and Mackay memorial hospital under Grant 100N2742E1, and in part by a General Research Fund of Hong Kong Research Grant Council (Project No. CUHK4441269).

[†]Chia-Hsiang Lin is with Institute of Communications Engineering, National Tsing Hua University, Hsinchu, Taiwan 30013, R.O.C. E-mail: chiahsiang.steven.lin@gmail.com, Tel: +886-3-5715131X34033, Fax: +886-3-5751787.

[‡]Wing-Kin Ma is with Department of Electronic Engineering, The Chinese University of Hong Kong, Shatin, N.T., Hong Kong. E-mail: wkma@ieee.org, Tel: +852-31634350, Fax: +852-26035558.

^{*}Wei-Chiang Li is with Institute of Communications Engineering, National Tsing Hua University, Hsinchu, Taiwan 30013, R.O.C. E-mail: weichiang-li@gmail.com, Tel: +886-3-5715131X34033, Fax: +886-3-5751787.

[§]Chong-Yung Chi is the corresponding author. Address: Institute of Communications Engineering & Department of Electrical Engineering, National Tsing Hua University, Hsinchu, Taiwan 30013, R.O.C. E-mail: cy-chi@ee.nthu.edu.tw, Tel: +886-3-5731156, Fax: +886-3-5751787.

[◇]ArulMurugan Ambikapathi is with Institute of Communications Engineering, National Tsing Hua University, Hsinchu, Taiwan 30013, R.O.C. E-mail: aareul@ieee.org, Tel: +886-3-5715131X34033, Fax: +886-3-5751787.

in [18] should also be noted. We should further mention that MVES also finds application in analytical chemistry [19], and that fundamentally MVES has a strong link to stochastic maximum-likelihood estimation [20].

What makes MVES special is that it seems to perform well even in the absence of pure pixels, i.e., pixels that are solely contributed by a single endmember. To be more accurate, extensive simulations found that MVES may estimate the ground-truth endmembers quite accurately in the noiseless case and without the pure-pixel assumption; see, e.g., [6], [20], [21]. At this point we should mention that while the pure-pixel assumption is elegant and has been exploited by some other approaches, such as simplex volume maximization (also [7] for a more recent work on near-separable non-negative matrix factorization), to arrive at remarkably simple blind HU algorithms, it is also an arguably restrictive assumption in general. In the HU context it has been suspected that MVES should be resistant to lack of pure pixels, but it is not known to what extent MVES can guarantee perfect endmember identifiability under no pure pixels. Hence, we depart from existing MVES works, wherein improved algorithm designs are usually the theme, and ask the following questions: can the endmember identifiability of the MVES criterion in the no pure-pixel case be *theoretically* pinned down? If yes, how bad (in terms of how heavy the data are mixed) can MVES withstand and where is the limit?

The contribution of this paper is theoretical. We aim to address the aforementioned questions through analysis. Previously, identifiability analysis for MVES was done only for the pure-pixel case in [6], and for the three endmember case in the preliminary version of this paper [22]. This paper considers the no pure-pixel case for any number of endmembers. We prove that MVES can indeed guarantee exact and unique recovery of the endmembers. The key condition for attaining such exact identifiability is that some measures concerning the pixels' purity and geometry (to be defined in Section III-A) have to be above a certain limit. The condition mentioned above is equivalent to the pure-pixel assumption for the case of two endmembers, and is much milder than the pure-pixel assumption for the case of three endmembers or more. Numerical experiments will be conducted to support the above claims.

This paper is organized as follows. The problem statement is described in Section II. The MVES identifiability analysis results and the associated proofs are given in Sections III and IV, respectively. Numerical results are provided in Section V to support our theoretical claims, and we conclude the paper in Section VI.

Notations: \mathbb{R}^n and $\mathbb{R}^{m \times n}$ denote the sets of all real-valued n -dimensional vectors and m -by- n matrices, respectively (resp.); $\|\cdot\|$ denotes the Euclidean norm of a vector; \mathbf{x}^T denotes the transpose of \mathbf{x} and the same applies to matrices; given a set $\mathcal{A} \subseteq \mathbb{R}^n$, we denote $\text{aff}\mathcal{A}$ and $\text{conv}\mathcal{A}$ as the affine hull and convex hull of \mathcal{A} , resp. (see [23]), $\text{int}\mathcal{A}$ and $\text{bd}\mathcal{A}$ as the interior and boundary of \mathcal{A} , resp., and $\text{vol}\mathcal{A}$ as the volume of \mathcal{A} ; the dimension of a set $\mathcal{A} \subseteq \mathbb{R}^n$ is defined as the affine dimension of $\text{aff}\mathcal{A}$; $\mathbf{x} \geq \mathbf{0}$ means that \mathbf{x} is elementwise non-negative; \mathbf{I} and $\mathbf{1}$ denote an identity matrix and all-one vector

of appropriate dimension, resp.; \mathbf{e}_i denotes a unit vector whose i th element is $[\mathbf{e}_i]_i = 1$ and j th element is $[\mathbf{e}_i]_j = 0$ for all $j \neq i$.

II. PROBLEM STATEMENT

In this section we review the background of the MVES identifiability analysis challenge.

A. Preliminaries

Before describing the problem, some basic facts about simplex should be mentioned. A convex hull

$$\text{conv}\{\mathbf{b}_1, \dots, \mathbf{b}_N\} = \left\{ \mathbf{x} = \sum_{i=1}^N \theta_i \mathbf{b}_i \mid \boldsymbol{\theta} \geq \mathbf{0}, \mathbf{1}^T \boldsymbol{\theta} = 1 \right\},$$

where $\mathbf{b}_1, \dots, \mathbf{b}_N \in \mathbb{R}^M$, $M \geq N - 1$, is called an $(N - 1)$ -dimensional simplex if $\mathbf{b}_1, \dots, \mathbf{b}_N$ are affinely independent. The volume of a simplex can be determined by [24]

$$\text{vol}(\text{conv}\{\mathbf{b}_1, \dots, \mathbf{b}_N\}) = \frac{1}{(N - 1)!} \sqrt{\det(\bar{\mathbf{B}}^T \bar{\mathbf{B}})}, \quad (1)$$

where $\bar{\mathbf{B}} = [\mathbf{b}_1 - \mathbf{b}_N, \mathbf{b}_2 - \mathbf{b}_N, \dots, \mathbf{b}_{N-1} - \mathbf{b}_N] \in \mathbb{R}^{M \times (N-1)}$. A simplex is called regular if the distances between any two vertices are the same.

B. Blind HU Problem Setup

We adopt a standard blind HU problem formulation (readers are referred to the literature, e.g., [3], [4], for coverage of the underlying modeling aspects). Concisely, consider a hyperspectral scene wherein the observed pixels can be modeled as linear mixtures of endmember spectral signatures

$$\mathbf{x}_n = \mathbf{A} \mathbf{s}_n, \quad n = 1, \dots, L, \quad (2)$$

where $\mathbf{x}_n \in \mathbb{R}^M$ denotes the n th pixel vector of the observed hyperspectral image, with M being the number of spectral bands; $\mathbf{A} = [\mathbf{a}_1, \dots, \mathbf{a}_N] \in \mathbb{R}^{M \times N}$ is the endmember signature matrix, with N being the number of endmembers; $\mathbf{s}_n \in \mathbb{R}^M$ is the abundance vector of the n th pixel; L is the number of pixels. The problem is to identify the unknown \mathbf{A} from the observations $\mathbf{x}_1, \dots, \mathbf{x}_L$, thereby allowing us to unmix the abundances (also unknown) blindly. To facilitate the subsequent problem description, the noiseless case is assumed. The following assumptions are standard in the blind HU context and will be assumed throughout the paper: (i) every abundance vector satisfies $\mathbf{s}_n \geq \mathbf{0}$ and $\mathbf{1}^T \mathbf{s}_n = 1$ (i.e., the abundance non-negativity and sum-to-one constraints); (ii) \mathbf{A} has full column rank; (iii) $[\mathbf{s}_1, \dots, \mathbf{s}_L]$ has full row rank; (iv) N is known.

C. Minimum-Volume Enclosing Simplex

This paper concentrates on the MVES approach for blind HU. MVES was inspired by the following intuition [9]: if we can find a simplex that circumscribes the data points $\mathbf{x}_1, \dots, \mathbf{x}_L$ and yields the minimum volume, then the vertices of such a simplex should be identical to, or close to, the true endmember spectral signatures $\mathbf{a}_1, \dots, \mathbf{a}_N$ themselves.

Figure 1 shows an illustration for the aforementioned intuition. Mathematically, the MVES criterion can be formulated as an optimization problem

$$\begin{aligned} \min_{\mathbf{b}_1, \dots, \mathbf{b}_N \in \mathbb{R}^M} \quad & \text{vol}(\text{conv}\{\mathbf{b}_1, \dots, \mathbf{b}_N\}) \\ \text{s.t.} \quad & \mathbf{x}_n \in \text{conv}\{\mathbf{b}_1, \dots, \mathbf{b}_N\}, \quad n = 1, \dots, L, \end{aligned} \quad (3)$$

wherein the solution of problem (3) is used as an estimate of \mathbf{A} . Problem (3) is NP-hard in general [25]; this means that the optimal MVES solution is unlikely to be computationally tractable for any arbitrarily given $\{\mathbf{x}_n\}_{n=1}^L$. Notwithstanding, it was found that carefully designed algorithms for handling problem (3), though being generally suboptimal in view of the NP-hardness of problem (3), can practically yield satisfactory endmember identification performance; see, e.g., [6], [8], [19], [20], and also [14], [16]–[18] for the noisy case. In this paper, we do not consider MVES algorithm design. Instead, we study the following fundamental, and very important, question: *When will the MVES problem (3) provide an optimal solution that is exactly and uniquely given by the true endmember matrix \mathbf{A} (up to a permutation)?*

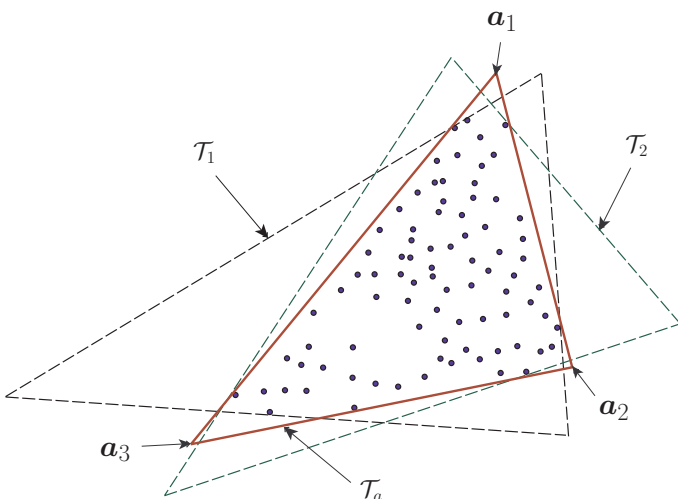


Fig. 1. A geometrical illustration of MVES. The dots are the data points $\{\mathbf{x}_n\}$, the number of endmembers is $N = 3$, and \mathcal{T}_1 , \mathcal{T}_2 and \mathcal{T}_a are data-enclosing simplices. In particular, \mathcal{T}_a is actually given by $\mathcal{T}_a = \text{conv}\{\mathbf{a}_1, \mathbf{a}_2, \mathbf{a}_3\}$. Visually, it can be seen that \mathcal{T}_a has a smaller volume than \mathcal{T}_1 and \mathcal{T}_2 .

It is known that MVES uniquely identifies \mathbf{A} if the pure-pixel assumption holds [6], that is, if, for each $i \in \{1, \dots, N\}$, there exists an abundance vector \mathbf{s}_n such that $\mathbf{s}_n = \mathbf{e}_i$. However, empirical evidence has suggested that even when the pure-pixel assumption does not hold, MVES (more precisely, approximate MVES by the existing algorithms) may still be able to uniquely identify \mathbf{A} . In this paper, we aim at analyzing the endmember identifiability of MVES in the no pure-pixel case.

III. MAIN RESULTS

This section describes the main results of our MVES identifiability analysis. As will be seen soon, MVES identifiability in the no pure-pixel case depends much on the level of “pixel

purity” of the observed data set. To this end, we need to precisely quantify what “pixel purity” is. The first subsection will introduce two pixel purity measures. The second subsection will then present the main results, and the third subsection will discuss their practical implications.

A. Pixel Purity Measures

A natural way to quantify pixel purity is to use the following measure

$$\rho = \max_{n=1, \dots, L} \|\mathbf{s}_n\|. \quad (4)$$

Eq. (4) will be called the *best pixel purity level* in the sequel. A large value of ρ implies that there exist abundance vectors whose purity is high, while a small value of ρ indicates more heavily mixed data. To see it, observe that $\|\mathbf{s}\| \leq 1$ for any $\mathbf{s} \geq \mathbf{0}$, $\mathbf{1}^T \mathbf{s} = 1$, and equality holds if and only if $\mathbf{s} = \mathbf{e}_k$ for any k ; that is, a pure pixel. Moreover, it can be shown that $\frac{1}{\sqrt{N}} \leq \|\mathbf{s}\|$ for any $\mathbf{s} \geq \mathbf{0}$, $\mathbf{1}^T \mathbf{s} = 1$, and equality holds if and only if $\mathbf{s} = \frac{1}{N} \mathbf{1}$; that is, a heavily mixed pixel. Without loss of generality (w.l.o.g.), we may assume

$$\frac{1}{\sqrt{N}} < \rho \leq 1,$$

where we rule out $\rho = \frac{1}{\sqrt{N}}$, which implies $\mathbf{s}_1 = \dots = \mathbf{s}_L = \frac{1}{N} \mathbf{1}$ and leads to a pathological case.

The previously defined pixel purity level reflects the best abundance purity among all the pixels, but says little on how the pixels are spread geometrically with respect to (w.r.t.) the various endmembers. We will also require another measure, defined as follows

$$\gamma = \sup\{r \leq 1 \mid \mathcal{R}(r) \subseteq \text{conv}\{\mathbf{s}_1, \dots, \mathbf{s}_L\}\}, \quad (5)$$

where

$$\begin{aligned} \mathcal{R}(r) &= \{\mathbf{s} \in \text{conv}\{\mathbf{e}_1, \dots, \mathbf{e}_N\} \mid \|\mathbf{s}\| \leq r\} \\ &= \{\mathbf{s} \in \mathbb{R}^N \mid \|\mathbf{s}\| \leq r\} \cap \text{conv}\{\mathbf{e}_1, \dots, \mathbf{e}_N\}. \end{aligned} \quad (6)$$

We call (5) the *uniform pixel purity level*; the reason for this will be illustrated soon. It can be shown that

$$\frac{1}{\sqrt{N}} \leq \gamma \leq \rho.$$

Also, if $\gamma = 1$, then the pure-pixel assumption is shown to hold.

To understand the differences between the pixel purity measures in (4) and (5), we first illustrate how $\mathcal{R}(r)$ looks like in Figure 2. As can be seen (and as will be shown), $\mathcal{R}(r)$ is a ball on the affine hull $\text{aff}\{\mathbf{e}_1, \dots, \mathbf{e}_N\}$ if $r \leq 1/\sqrt{N-1}$. Otherwise, $\mathcal{R}(r)$ takes a shape like a vertices-cropped version of the unit simplex $\text{conv}\{\mathbf{e}_1, \dots, \mathbf{e}_N\}$. In addition, it can be shown that (4) equals

$$\rho = \inf\{r \mid \text{conv}\{\mathbf{s}_1, \dots, \mathbf{s}_L\} \subseteq \mathcal{R}(r)\}.$$

In Figure 3, we give several examples with the abundances. From the figures, an interesting observation is that $\mathcal{R}(\rho)$ serves as a smallest $\mathcal{R}(r)$ that circumscribes the abundance convex hull $\text{conv}\{\mathbf{s}_1, \dots, \mathbf{s}_L\}$, while $\mathcal{R}(\gamma)$ serves as a largest $\mathcal{R}(r)$ that is inscribed in $\text{conv}\{\mathbf{s}_1, \dots, \mathbf{s}_L\}$. Moreover, we see that

if the abundances are spread in a relatively symmetric manner w.r.t. all the endmembers, then ρ and γ are similar; this is the case with Figures 3(a)-3(c). However, ρ and γ can be quite different if the abundances are asymmetrically spread; this is the case with Figure 3(d) where some endmembers have pixels of high purity but some do not. Hence, the uniform pixel purity level γ quantifies a pixel purity level that applies uniformly to *all* the endmembers, not just to the best.

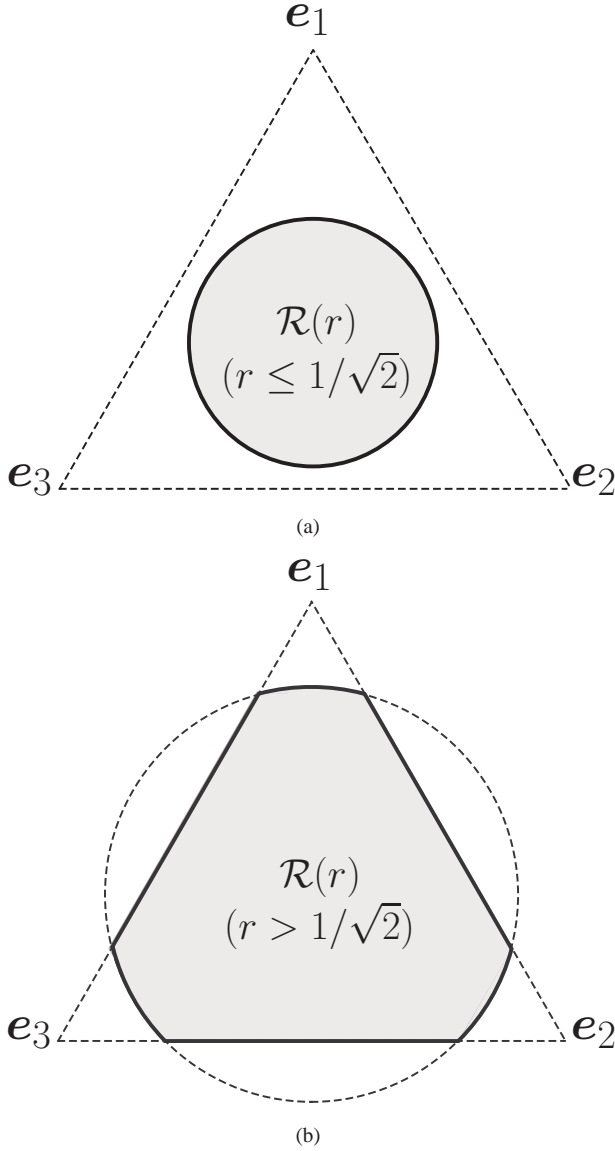


Fig. 2. A geometrical illustration of $\mathcal{R}(r)$ in (6) for $N = 3$. We view $\mathcal{R}(r)$ by adjusting the viewpoint to be perpendicular to the affine hull of $\{e_1, e_2, e_3\}$.

B. Provable MVES Identifiability

Our provable MVES identifiability results are described as follows. To facilitate our analysis, consider the following definition.

Definition 1 (minimum volume enclosing simplex) Given an m -dimensional set $\mathcal{U} \subseteq \mathbb{R}^n$, the notation $\text{MVES}(\mathcal{U})$

denotes the set that collects all m -dimensional minimum volume simplices that enclose \mathcal{U} and lie in $\text{aff}\mathcal{U}$.

Now, let

$$\begin{aligned} \mathcal{T}_e &= \text{conv}\{e_1, \dots, e_N\} \subseteq \mathbb{R}^N, \\ \mathcal{T}_a &= \text{conv}\{a_1, \dots, a_N\} \subseteq \mathbb{R}^M, \end{aligned}$$

denote the $(N-1)$ -dimensional unit simplex and the endmembers' simplex, respectively. Also, for convenience, let

$$\mathcal{X}_L = \{\mathbf{x}_1, \dots, \mathbf{x}_L\}, \quad \mathcal{S}_L = \{\mathbf{s}_1, \dots, \mathbf{s}_L\},$$

denote the sets of all the observed hyperspectral pixels and abundance vectors, resp., and note their dependence $\mathbf{x}_n = \mathbf{A}\mathbf{s}_n$ as described in (2). Under the above definition, the exact and unique identifiability problem of the MVES criterion in (3) can be posed as a problem of finding conditions under which

$$\text{MVES}(\mathcal{X}_L) = \{\mathcal{T}_a\}.$$

Our first result reveals that the MVES perfect identifiability does not depend on \mathbf{A} (as far as \mathbf{A} has full column rank):

Proposition 1 $\text{MVES}(\mathcal{X}_L) = \{\mathcal{T}_a\}$ if and only if $\text{MVES}(\mathcal{S}_L) = \{\mathcal{T}_e\}$.

The proof of Proposition 1, as well as those of the theorems to be presented, will be provided in the next section. Proposition 1 suggests that to analyze the perfect MVES identifiability w.r.t. the observed pixel vectors, it is equivalent to analyze the perfect MVES identifiability w.r.t. the abundance vectors. One may expect that perfect identifiability cannot be achieved for too heavily mixed pixels. We prove that this is indeed true.

Theorem 1 Assume $N \geq 3$. If $\text{MVES}(\mathcal{S}_L) = \{\mathcal{T}_e\}$, then the best pixel purity level must satisfy $\rho > \frac{1}{\sqrt{N-1}}$.

To get some idea, consider the example in Figure 3(a). Since Figure 3(a) does not satisfy the condition in Theorem 1, it fails to provide exact recovery of the true endmembers. Theorem 1 is only a necessary perfect identifiability condition. We also prove a sufficient perfect identifiability condition, described as follows:

Theorem 2 Assume $N \geq 3$. If the uniform pixel purity level satisfies $\gamma > \frac{1}{\sqrt{N-1}}$, then $\text{MVES}(\mathcal{S}_L) = \{\mathcal{T}_e\}$.

Among the four examples in Figure 3, Figure 3(b) and Figure 3(c) are cases that satisfy the condition in Theorem 2 and achieve exact and unique recovery of the true endmembers.

It is worthwhile to emphasize that the sufficient identifiability condition in Theorem 2 is much milder than the pure-pixel assumption (which is equivalent to $\gamma = 1$) for $N \geq 3$. In fact, the pixel purity requirement $1/\sqrt{N-1}$ diminishes as N increases—which seems to suggest that MVES can handle more heavily mixed cases as the number of endmembers increases. Thus, Theorem 2 provides a theoretical justification on the robustness of MVES against lack of pure pixels.

One may be curious about how Theorem 2 is proven. Essentially, the idea lies in finding a connection between the

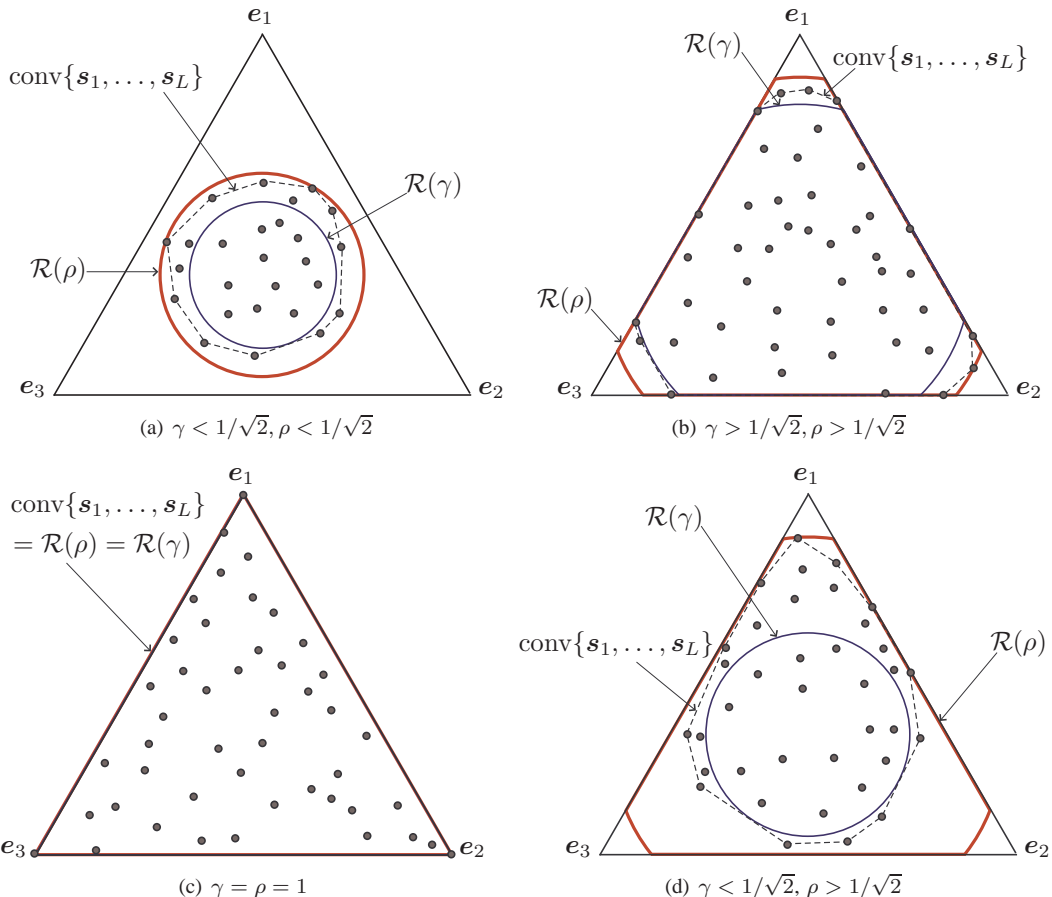


Fig. 3. Examples with the abundance distributions and the corresponding best and uniform pixel purity levels.

MVES identifiability conditions of \mathcal{S}_L and $\mathcal{R}(\gamma)$ [cf. (5)-(6)]. In particular, it is shown that if $\text{MVES}(\mathcal{R}(\gamma)) = \{\mathcal{T}_e\}$, then $\text{MVES}(\mathcal{S}_L) = \{\mathcal{T}_e\}$. Subsequently, the problem is to pin down the MVES identifiability condition of $\mathcal{R}(r)$. This turns out to be the core part of our analysis, and the result is as follows.

Theorem 3 *For any $1/\sqrt{N-1} < r \leq 1$, we have $\text{MVES}(\mathcal{R}(r)) = \{\mathcal{T}_e\}$; i.e., there is only one MVES of $\mathcal{R}(r)$ for $1/\sqrt{N-1} < r \leq 1$ and that MVES is always given by the unit simplex.*

As an example, Fig. 2.(b) is an instance where Theorem 3 holds; by visual observation of Fig. 2.(b), we may argue that the MVES of $\mathcal{R}(r)$ for $N = 3$ and $r > 1/\sqrt{2}$ should be the unit simplex. Also, we should note that the geometric problem in Theorem 3 is interesting in its own right, and the result could be of independent interest in other fields.

Before we finish this subsection, we should mention the case of $N = 2$. While the number of endmembers in practical scenarios is often a lot more than two, it is still interesting to know the identifiability for $N = 2$.

Proposition 2 *Assume $N = 2$. We have $\text{MVES}(\mathcal{S}_L) = \{\mathcal{T}_e\}$ if and only if the pure-pixel assumption holds.*

We should recall that the pure-pixel assumption corresponds to $\gamma = 1$.

C. Further Discussion

We have seen that the uniform pixel purity level γ provides a key quantification on when MVES achieves perfect endmember identifiability. Nevertheless, one may have these further questions: How is γ related to the abundance pixel set \mathcal{S}_L exactly? Can the relationship be characterized in an explicit and practically interpretable manner? For example, as can be observed in the three-endmember illustrations in Fig. 3, satisfying the sufficient identifiability condition $\gamma > 1/\sqrt{N-1}$ in Theorem 2 seems to require some abundance pixels to lie on the boundary of \mathcal{T}_e . However, from the definition of γ in (5), it is not immediately clear how such a result can be deduced (e.g., how many pixels on the boundary, and which parts of the boundary?). Unfortunately, explicit characterization of γ w.r.t. \mathcal{S}_L appears to be a difficult analysis problem. In fact, even computing the value of γ for a given \mathcal{S}_L is generally a computationally hard problem¹ [26].

Despite the aforementioned analysis bottleneck, our empirical experience suggests that if every s_n follows a continuous distribution that has a support covering $\mathcal{R}(r)$ for $r > 1/\sqrt{N-1}$ (e.g., Dirichlet distributions), and the number of pixels L is large, there is a large probability for MVES

¹More accurately, verifying whether or not a convex body ($\mathcal{R}(r)$ here) belongs to a \mathcal{V} -polytope ($\text{conv}\mathcal{S}_L$ here) has been shown to be coNP-complete [26].

to achieve perfect identifiability. The numerical results in Section V will support this. Moreover, we can study special, but still meaningful, cases. Herein we show one that uses the following assumption:

Assumption 1 For every $i, j \in \{1, \dots, N\}$, $i \neq j$, there exists a pixel, whose index is denoted by $n(i, j)$, such that its abundance vector takes the form

$$\mathbf{s}_{n(i,j)} = \alpha_{ij} \mathbf{e}_i + (1 - \alpha_{ij}) \mathbf{e}_j, \quad (7)$$

for some coefficient α_{ij} that satisfies $\frac{1}{2} < \alpha_{ij} \leq 1$.

Assumption 1 means that we can find pixels that are constituted by two endmembers, with one dominating another as determined by the coefficient $\alpha_{ij} > \frac{1}{2}$. Also, the pixels in (7) lie on the edges of \mathcal{T}_e . Fig. 4 gives an illustration for $N = 3$. Note that Assumption 1 reduces to the pure-pixel assumption if $\alpha_{ij} = 1$ for all i, j . Hence, Assumption 1 may be seen as a more general assumption than the pure-pixel assumption. In the example of $N = 3$ in Fig. 4, we see that γ should increase as α_{ij} 's increase. In fact, this can be proven to be true for any $N \geq 2$.

Theorem 4 Under Assumption 1 and for $N \geq 2$, the uniform pixel purity level satisfies

$$\gamma \geq \sqrt{\frac{1}{N} \left[\frac{(N\alpha - 1)^2}{N - 1} + 1 \right]},$$

where

$$\alpha = \min_{\substack{i,j \in \{1, \dots, N\} \\ i \neq j}} \alpha_{ij}$$

is the smallest value of α_{ij} 's.

The proof of Theorem 4 is given in Section IV-F. Theorem 4 is useful in the following way. If we compare Theorems 2 and 4, we see that the condition

$$\sqrt{\frac{1}{N} \left[\frac{(N\alpha - 1)^2}{N - 1} + 1 \right]} > \frac{1}{\sqrt{N-1}},$$

implies exact unique identifiability of MVES. It is shown that the above equation is equivalent to

$$\alpha > \frac{2}{N},$$

for $N \geq 3$. By also noting $\frac{1}{2} < \alpha \leq 1$ in Assumption 1, and the fact that $\frac{1}{2} \geq \frac{2}{N}$ for $N \geq 4$, we have the following conclusion.

Corollary 1 Suppose that Assumption 1 holds. For $N = 3$, the exact unique identifiability condition $\text{MVES}(\mathcal{S}_L) = \{\mathcal{T}_e\}$ is achieved if $\alpha_{ij} > \frac{2}{3}$ for all i, j . For $N \geq 4$, the condition $\text{MVES}(\mathcal{S}_L) = \{\mathcal{T}_e\}$ is always achieved (subject to $\frac{1}{2} < \alpha_{ij} \leq 1$ in Assumption 1).

The implication of Corollary 1 is particularly interesting for $N \geq 4$ —MVES for $N \geq 4$ always provides perfect identifiability under Assumption 1. However, we should also note that this result is under the premise of Assumption 1. In

particular, it is seen that to satisfy Assumption 1 for general α_{ij} 's, the number of pixels L should be no less than $N(N-1)$. This implies that we would need more pixels to achieve perfect MVES identifiability as N increases.

We finish with mentioning some arising open problems. From the above discussion, it is natural to further question whether (7) in Assumption 1 can be relaxed to combinations of three endmembers, or more. Also, the whole work has so far assumed the noiseless case, and sensitivity in the noisy case has not been touched. These challenges are left as future work.

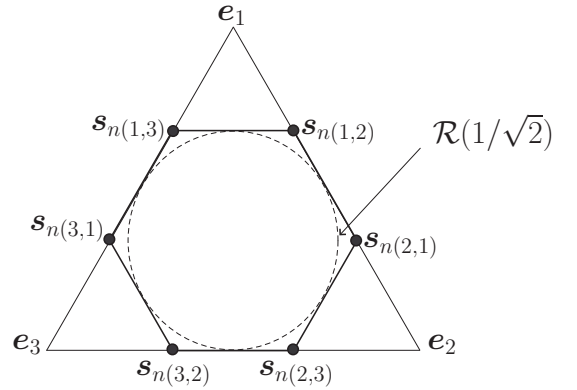


Fig. 4. Illustration of Assumption 1. $N = 3$, $\alpha_{ij} = 2/3$ for all i, j .

IV. PROOF OF THE MAIN RESULTS

This section provides the proof of the main results described in the previous section. Readers who are more interested in numerical experiments may jump to Section V.

A. Proof of Proposition 1

The following lemma will be used to prove Proposition 1:

Lemma 1 Let $f(\mathbf{x}) = \mathbf{A}\mathbf{x}$, where $\mathbf{A} \in \mathbb{R}^{M \times N}$, $M \geq N$, and suppose that \mathbf{A} has full column rank.

(a) Let $\mathcal{T}_G \subset \mathbb{R}^N$ be an $(N-1)$ -dimensional simplex, and suppose $\mathcal{T}_G \subset \text{aff}\{\mathbf{e}_1, \dots, \mathbf{e}_N\}$. We have

$$\text{vol}(f(\mathcal{T}_G)) = \alpha \cdot \text{vol}(\mathcal{T}_G), \quad (8)$$

where $\alpha = \sqrt{\frac{\det(\bar{\mathbf{A}}^T \bar{\mathbf{A}})}{N}}$, and $\bar{\mathbf{A}} = [\mathbf{a}_1 - \mathbf{a}_N, \mathbf{a}_2 - \mathbf{a}_N, \dots, \mathbf{a}_{N-1} - \mathbf{a}_N]$. Also, it holds true that $f(\mathcal{T}_G) \subset \text{aff}\{\mathbf{a}_1, \dots, \mathbf{a}_N\}$.

(b) Let $\mathcal{T}_H \subset \mathbb{R}^M$ be an $(N-1)$ -dimensional simplex, and suppose $\mathcal{T}_H \subset \text{aff}\{\mathbf{a}_1, \dots, \mathbf{a}_N\}$. We have

$$\text{vol}(f^{-1}(\mathcal{T}_H)) = \frac{1}{\alpha} \cdot \text{vol}(\mathcal{T}_H), \quad (9)$$

and $f^{-1}(\mathcal{T}_H) \subset \text{aff}\{\mathbf{e}_1, \dots, \mathbf{e}_N\}$.

The proof of Lemma 1 is relegated to Appendix A. Now, suppose that $\text{MVES}(\mathcal{S}_L) = \{\mathcal{T}_e\}$, but $\text{MVES}(\mathcal{X}_L) \neq \{\mathcal{T}_a\}$. Let \mathcal{T}_H be an MVES of \mathcal{X}_L . By the MVES definition (see Definition 1), we have

$$\mathcal{X}_L \subseteq \mathcal{T}_H, \quad \mathcal{T}_H \subseteq \text{aff}\{\mathbf{x}_1, \dots, \mathbf{x}_L\}, \quad (10)$$

$$\text{vol}(\mathcal{T}_H) \leq \text{vol}(\mathcal{T}_a).$$

Recall that $[s_1, \dots, s_L]$ is assumed to have full row rank and satisfy $\mathbf{1}^T s_n = 1$ for all n . From these assumptions, one can prove that $\text{aff}\{s_1, \dots, s_L\} = \text{aff}\{e_1, \dots, e_N\}$, and $\text{aff}\{x_1, \dots, x_L\} = \text{aff}\{a_1, \dots, a_N\}$; see [27, Lemma 1] for example. Then, by applying Lemma 1.(b) to (10), we obtain

$$\begin{aligned} \mathcal{S}_L &\subseteq f^{-1}(\mathcal{T}_H), \quad f^{-1}(\mathcal{T}_H) \subseteq \text{aff}\{e_1, \dots, e_N\}, \\ \text{vol}(f^{-1}(\mathcal{T}_H)) &\leq \text{vol}(f^{-1}(\mathcal{T}_a)) = \text{vol}(\mathcal{T}_e). \end{aligned}$$

The above equation implies that \mathcal{T}_e is not the only MVES of \mathcal{S}_L , which is a contradiction.

On the other hand, suppose that $\text{MVES}(\mathcal{X}_L) = \{\mathcal{T}_a\}$, but $\text{MVES}(\mathcal{S}_L) \neq \{\mathcal{T}_e\}$. This statement can be shown to be a contradiction, by the same proof as above (particularly, the incorporation of Lemma 1.(a)). The proof of Proposition 1 is therefore complete.

B. Proof of Theorem 1

The proof is done by contradiction. Suppose that $\text{MVES}(\mathcal{S}_L) = \{\mathcal{T}_e\}$, but $\rho \leq \frac{1}{\sqrt{N-1}}$. Recall

$$\mathcal{R}(r) = \mathcal{T}_e \cap \{s \in \mathbb{R}^N \mid \|s\| \leq r\}. \quad (11)$$

The proof is divided into four steps.

Step 1: We show that any $\mathcal{V} \in \text{MVES}(\mathcal{R}(\rho))$ is also an MVES of \mathcal{S}_L . To prove it, note that

$$\mathcal{S}_L \subseteq \mathcal{R}(\rho). \quad (12)$$

Eq. (12) implies that

$$\text{vol}(\mathcal{U}) \leq \text{vol}(\mathcal{V}), \quad \text{for all } \mathcal{U} \in \text{MVES}(\mathcal{S}_L), \mathcal{V} \in \text{MVES}(\mathcal{R}(\rho)). \quad (13)$$

Also, since \mathcal{T}_e encloses $\mathcal{R}(\rho)$, we have

$$\text{vol}(\mathcal{V}) \leq \text{vol}(\mathcal{T}_e), \quad \text{for all } \mathcal{V} \in \text{MVES}(\mathcal{R}(\rho)). \quad (14)$$

Since we assume $\text{MVES}(\mathcal{S}_L) = \{\mathcal{T}_e\}$ in the beginning, we observe from (13) and (14) that $\text{vol}(\mathcal{U}) = \text{vol}(\mathcal{V})$ for all $\mathcal{U} \in \text{MVES}(\mathcal{S}_L)$, $\mathcal{V} \in \text{MVES}(\mathcal{R}(\rho))$. The above equality, together with (12), implies that any $\mathcal{V} \in \text{MVES}(\mathcal{R}(\rho))$ is an MVES of \mathcal{S}_L (or satisfies $\mathcal{V} \in \text{MVES}(\mathcal{S}_L)$).

Step 2: We give an alternative representation of $(N-1)$ -dimensional simplices on $\text{aff}\{e_1, \dots, e_N\}$, which will facilitate the proof. The affine hull $\text{aff}\{e_1, \dots, e_N\}$ can be equivalently expressed as

$$\text{aff}\{e_1, \dots, e_N\} = \{s = C\theta + d \mid \theta \in \mathbb{R}^{N-1}\}, \quad (15)$$

where

$$d = \frac{1}{N} \sum_{i=1}^N e_i = \frac{1}{N} \mathbf{1},$$

and $C \in \mathbb{R}^{N \times (N-1)}$ is the first $N-1$ principal left singular vectors of $R = [e_1 - d, \dots, e_N - d]$; see [6], [27]. We note that

$$R = I - \frac{1}{N} \mathbf{1}\mathbf{1}^T,$$

which, as a standard matrix result, its first $N-1$ principal left singular vector can be shown to be any C such that

$$U = \left[C, \frac{1}{\sqrt{N}} \mathbf{1} \right] \quad (16)$$

is a unitary matrix. Or, equivalently, C is any semi-unitary matrix such that $C^T d = \mathbf{0}$.

Recall that an $(N-1)$ -dimensional simplex $\mathcal{V} \subseteq \text{aff}\{e_1, \dots, e_N\}$ can be written as

$$\mathcal{V} = \text{conv}\{v_1, \dots, v_N\},$$

where $v_i \in \text{aff}\{e_1, \dots, e_N\}$ for all i . By (15), each $v_i \in \text{aff}\{e_1, \dots, e_N\}$ can be represented by $v_i = Cw_i + d$ for some $w_i \in \mathbb{R}^{N-1}$. Applying this result to $\text{conv}\{v_1, \dots, v_N\}$, we obtain the following equivalent representation of \mathcal{V}

$$\mathcal{V} = \{s = C\theta + d \mid \theta \in \mathcal{W}\}, \quad (17)$$

where

$$\mathcal{W} = \text{conv}\{w_1, \dots, w_N\}. \quad (18)$$

Also, by the simplex volume formula (1) and the semi-unitarity of C , the following relation is shown

$$\text{vol}(\mathcal{V}) = \text{vol}(\mathcal{W}). \quad (19)$$

Step 3: We show that there are infinitely many MVES of $\mathcal{R}(\rho)$ for $\frac{1}{\sqrt{N}} < \rho \leq \frac{1}{\sqrt{N-1}}$. Consider the following lemma.

Lemma 2 *Let*

$$\mathcal{C}(r) = \text{aff}\{e_1, \dots, e_N\} \cap \{s \in \mathbb{R}^N \mid \|s\| \leq r\}. \quad (20)$$

denote a 2-norm ball on $\text{aff}\{e_1, \dots, e_N\}$. If $\frac{1}{\sqrt{N}} < r \leq \frac{1}{\sqrt{N-1}}$, then $\mathcal{R}(r)$ in (11) equals $\mathcal{C}(r)$.

Proof of Lemma 2: Note that $\mathcal{R}(r) \subseteq \mathcal{C}(r)$. Hence, to prove Lemma 2, it suffices to show that $\mathcal{C}(r) \subseteq \mathcal{R}(r)$. By the equivalent affine hull representation in (15), we can write $\mathcal{C}(r) = \{s = C\theta + d \mid \|s\| \leq r\}$. By substituting $s = C\theta + d$ into $\|s\| \leq r$, we get, for any $s \in \mathcal{C}(r)$,

$$\|s\|^2 \leq r^2 \iff \|\theta\|^2 + \|d\|^2 \leq r^2 \quad (21a)$$

$$\iff \|\theta\|^2 \leq r^2 - \frac{1}{N}, \quad (21b)$$

where (21a) is obtained by using the orthogonality in (16); (21b) is by $\|d\|^2 = \frac{1}{N}$. Hence, $\mathcal{C}(r)$ can be rewritten as

$$\mathcal{C}(r) = \{s = C\theta + d \mid \|\theta\|^2 \leq r^2 - 1/N\}. \quad (22)$$

Moreover, by letting c^i and u^i denote the i th rows of C and U respectively, we have

$$s_i = [c^i]^T \theta + d_i \quad (23a)$$

$$\geq -\|c^i\| \|\theta\| + \frac{1}{N} \quad (23b)$$

$$\geq -\sqrt{\frac{N-1}{N}} \cdot \sqrt{\frac{1}{(N-1) \cdot N}} + \frac{1}{N} = 0, \quad (23c)$$

where (23b) is due to the Cauchy-Schwartz inequality; (23c) is due to (21b), $r \leq \frac{1}{\sqrt{N-1}}$, and the fact that $1 = \|u^i\|^2 = \frac{1}{N} + \|c^i\|^2$ (see (16) and note its orthogonality). Eq. (23) suggests that any $s \in \mathcal{C}(r)$ automatically satisfies $s \geq \mathbf{0}$, and hence, $s \in \mathcal{R}(r)$. We therefore conclude that $\mathcal{C}(r) = \mathcal{R}(r)$. ■

By Lemma 2, we can replace $\mathcal{R}(\rho)$ by $\mathcal{C}(\rho)$ and consider the MVES of the latter. Suppose that $\mathcal{V} \in \text{MVES}(\mathcal{C}(\rho))$. Our argument is that a suitably rotated version of \mathcal{V} is also an

MVES of $\mathcal{C}(\rho)$. To be precise, use the representation in (17)-(18) to describe \mathcal{V} . Comparing (17)-(18) and (22), we see that $\mathcal{C}(\rho) \subseteq \mathcal{V}$ is equivalent to

$$\{\boldsymbol{\theta} \mid \|\boldsymbol{\theta}\|^2 \leq \rho^2 - 1/N\} \subseteq \mathcal{W}. \quad (24)$$

From \mathcal{W} , let us construct another simplex

$$\mathcal{V}' = \{\mathbf{s} = \mathbf{C}\mathbf{Q}\boldsymbol{\theta} + \mathbf{d} \mid \boldsymbol{\theta} \in \mathcal{W}\}, \quad (25)$$

where $\mathbf{Q} \in \mathbb{R}^{(N-1) \times (N-1)}$ is a unitary matrix. Due to (24), \mathcal{V}' can be verified to satisfy $\mathcal{C}(\rho) \subseteq \mathcal{V}'$. Also, by observing the semi-unitarity of $\mathbf{C}\mathbf{Q}$, the volume of \mathcal{V}' is shown to equal

$$\text{vol}(\mathcal{V}') = \text{vol}(\mathcal{W}) = \text{vol}(\mathcal{V}).$$

In other words, \mathcal{V}' is also an MVES of $\mathcal{C}(\rho)$. In fact, the argument above holds for any unitary \mathbf{Q} . Since there are infinitely many unitary \mathbf{Q} for $N \geq 3$ (note that $\mathbf{Q} \in \mathbb{R}^{(N-1) \times (N-1)}$), we also have infinitely many MVESs of $\mathcal{C}(\rho)$ for $N \geq 3$.

Step 4: We combine the results in the above steps to draw conclusion. Step 1 shows that any $\mathcal{V} \in \text{MVES}(\mathcal{R}(\rho))$ is also an MVES of \mathcal{S}_L , while Step 3 shows that $\mathcal{R}(\rho)$ has infinitely many MVESs for $\rho \leq \frac{1}{\sqrt{N-1}}$, $N \geq 3$. This contradicts the assumption that there is only one MVES of \mathcal{S}_L . The proof of Theorem 1 is therefore complete.

C. Proof of Theorem 2

To facilitate our proof, let us introduce the following fact.

Fact 1 *Let $\mathcal{C}, \mathcal{D} \subseteq \mathbb{R}^n$ be two sets of identical dimension, with $\mathcal{C} \subseteq \mathcal{D}$. If $\mathcal{D} \subseteq \mathcal{T}$ for some $\mathcal{T} \in \text{MVES}(\mathcal{C})$, then $\mathcal{T} \in \text{MVES}(\mathcal{D})$ and $\text{MVES}(\mathcal{D}) \subseteq \text{MVES}(\mathcal{C})$.*

Proof of Fact 1: Note that $\mathcal{C} \subseteq \mathcal{D}$ implies that any $\mathcal{T}' \in \text{MVES}(\mathcal{D})$ is a simplex enclosing \mathcal{C} . Since \mathcal{T} is a minimum volume simplex among all the \mathcal{C} -enclosing simplices, we have

$$\text{vol}(\mathcal{T}) \leq \text{vol}(\mathcal{T}') \text{ for all } \mathcal{T}' \in \text{MVES}(\mathcal{D}). \quad (26)$$

Moreover, the condition $\mathcal{D} \subseteq \mathcal{T}$ implies that \mathcal{T} is also a \mathcal{D} -enclosing simplex, and, as a result, equality in (26) holds. It also follows that any $\mathcal{T}' \in \text{MVES}(\mathcal{D})$ is also an MVES of \mathcal{C} . ■

Now we proceed with the main proof.

Step 1: We show that

$$\mathcal{T}_e \in \text{MVES}(\mathcal{R}(r)), \text{ for any } r \geq \frac{1}{\sqrt{N-1}}. \quad (27)$$

Note from the definition of $\mathcal{R}(r)$ in (6) that

$$\mathcal{C}\left(\frac{1}{\sqrt{N-1}}\right) = \mathcal{R}\left(\frac{1}{\sqrt{N-1}}\right) \subseteq \mathcal{R}(r) \subseteq \mathcal{T}_e, \quad (28)$$

for any $r \in [1/\sqrt{N-1}, 1]$, where the first equality is by Lemma 2. We prove that

Lemma 3 *The unit simplex \mathcal{T}_e is an MVES of $\mathcal{C}(1/\sqrt{N-1})$.*

The proof of Lemma 3 is relegated to Appendix B. By applying Fact 1 and Lemma 3 to (28), we obtain $\mathcal{T}_e \in \text{MVES}(\mathcal{R}(r))$ for $r \in [1/\sqrt{N-1}, 1]$.

Step 2: We prove that

$$\text{MVES}(\mathcal{S}_L) \subseteq \text{MVES}(\mathcal{R}(\gamma)), \text{ for } \gamma \geq \frac{1}{\sqrt{N-1}}. \quad (29)$$

By the definition of γ in (5), we have

$$\mathcal{R}(\gamma) \subseteq \text{conv}\mathcal{S}_L \subseteq \mathcal{T}_e. \quad (30)$$

Also, in Step 1, it has been identified that $\mathcal{T}_e \in \text{MVES}(\mathcal{R}(r))$ for $r \in [1/\sqrt{N-1}, 1]$. Hence, for $\gamma \geq 1/\sqrt{N-1}$, we can apply Fact 1 to (30) to obtain

$$\text{MVES}(\text{conv}\mathcal{S}_L) \subseteq \text{MVES}(\mathcal{R}(\gamma)). \quad (31)$$

Next, we use a straightforward fact in convex analysis: for a convex set \mathcal{T} , the condition $\mathcal{C} \subseteq \mathcal{T}$ is the same as $\text{conv}\mathcal{C} \subseteq \mathcal{T}$, and vice versa. In the context here, this implies that any MVES of $\text{conv}\mathcal{S}_L$ also encloses \mathcal{S}_L , and the converse is also true. Hence, we have

$$\text{MVES}(\text{conv}\mathcal{S}_L) = \text{MVES}(\mathcal{S}_L). \quad (32)$$

By combining (31) and (32), Eq. (29) is obtained.

Step 3: We prove that

$$\text{MVES}(\mathcal{R}(\gamma)) = \{\mathcal{T}_e\}, \text{ for } \gamma > \frac{1}{\sqrt{N-1}}. \quad (33)$$

It has been shown in Step 1 that $\mathcal{T}_e \in \text{MVES}(\mathcal{R}(\gamma))$. The question is whether there exists another MVES $\mathcal{T}' \in \text{MVES}(\mathcal{R}(\gamma))$, with $\mathcal{T}' \neq \mathcal{T}_e$. By Theorem 3, such a \mathcal{T}' does not exist. Thus, (33) is obtained.

Step 4: We combine the results in Steps 2 and 3. Specifically, by (29) and (33), we get $\text{MVES}(\mathcal{S}_L) \subseteq \{\mathcal{T}_e\}$. As \mathcal{S}_L is enclosed by \mathcal{T}_e , we further deduce $\text{MVES}(\mathcal{S}_L) = \{\mathcal{T}_e\}$. Theorem 2 is therefore proven.

D. Proof of Theorem 3

Let $\mathcal{T}' \in \text{MVES}(\mathcal{R}(r))$ be an arbitrary MVES of $\mathcal{R}(r)$ for $1/\sqrt{N-1} < r \leq 1$. We prove Theorem 3 by showing that $\mathcal{T}' = \mathcal{T}_e$ is always true. The proof is divided into three steps.

Step 1: We show that

$$\mathcal{T}' \in \text{MVES}(\mathcal{R}(1/\sqrt{N-1})).$$

To prove this, note that $\mathcal{R}(1/\sqrt{N-1}) \subseteq \mathcal{R}(r)$ for all $1/\sqrt{N-1} \leq r \leq 1$. Also, it has been shown in (27) that $\mathcal{T}_e \in \text{MVES}(\mathcal{R}(r))$ for all $1/\sqrt{N-1} \leq r \leq 1$. Applying Fact 1 to the above two results yields

$$\text{MVES}(\mathcal{R}(r)) \subseteq \text{MVES}(\mathcal{R}(1/\sqrt{N-1})),$$

for all $1/\sqrt{N-1} \leq r \leq 1$. Since $\mathcal{T}' \in \text{MVES}(\mathcal{R}(r))$ for $1/\sqrt{N-1} < r \leq 1$, it follows that $\mathcal{T}' \in \text{MVES}(\mathcal{R}(1/\sqrt{N-1}))$ is also true.

Step 2: To proceed further, we apply the equivalent representation in (17)-(18) to rewrite \mathcal{T}_e as

$$\mathcal{T}_e = \{\mathbf{s} = \mathbf{C}\boldsymbol{\theta} + \mathbf{d} \mid \boldsymbol{\theta} \in \mathcal{W}_e\} \quad (34)$$

for some $(N-1)$ -dimensional simplex $\mathcal{W}_e \subseteq \mathbb{R}^{N-1}$. Similarly, we can characterize \mathcal{T}' by

$$\mathcal{T}' = \{\mathbf{s} = \mathbf{C}\boldsymbol{\theta} + \mathbf{d} \mid \boldsymbol{\theta} \in \mathcal{W}'\} \quad (35)$$

for some $(N-1)$ -dimensional simplex $\mathcal{W}' \subseteq \mathbb{R}^{N-1}$. Also, by noting $\mathcal{R}(r) = \mathcal{T}_e \cap \mathcal{C}(r)$, the expression of $\mathcal{C}(r)$ in (22), and $\mathcal{R}(r) = \mathcal{C}(r)$ for $r = 1/\sqrt{N-1}$ (see Lemma 2), $\mathcal{R}(r)$ can be expressed as

$$\mathcal{R}(r) = \begin{cases} \{\mathbf{s} = \mathbf{C}\boldsymbol{\theta} + \mathbf{d} \mid \boldsymbol{\theta} \in \mathcal{B}(\sqrt{r^2 - 1/N})\}, & r = \frac{1}{\sqrt{N-1}} \\ \{\mathbf{s} = \mathbf{C}\boldsymbol{\theta} + \mathbf{d} \mid \boldsymbol{\theta} \in \mathcal{W}_e \cap \mathcal{B}(\sqrt{r^2 - 1/N})\}, & r > \frac{1}{\sqrt{N-1}} \end{cases} \quad (36)$$

where

$$\mathcal{B}(r) = \{\boldsymbol{\theta} \in \mathbb{R}^{N-1} \mid \|\boldsymbol{\theta}\| \leq r\}. \quad (37)$$

Now, by comparing (35)-(36), the following result can be proven:

$$\begin{aligned} \mathcal{T}' \in \text{MVES}(\mathcal{R}(r)) &\iff \\ \mathcal{W}' \in \begin{cases} \text{MVES}(\mathcal{B}(\sqrt{r^2 - 1/N})), & r = \frac{1}{\sqrt{N-1}} \\ \text{MVES}(\mathcal{W}_e \cap \mathcal{B}(\sqrt{r^2 - 1/N})), & r > \frac{1}{\sqrt{N-1}} \end{cases} & (38) \end{aligned}$$

The proof of (38) is analogous to that of Proposition 1, and will not be repeated here.

Step 3: From the equivalent representation (38), we further deduce the following results: i) $\mathcal{W}_e, \mathcal{W}' \in \text{MVES}(\mathcal{B}(\sqrt{r^2 - 1/N}))$ for $r = 1/\sqrt{N-1}$, which is due to Step 1 and (27); ii) $\mathcal{W}_e \cap \mathcal{B}(\sqrt{r^2 - 1/N}) \subseteq \mathcal{W}'$ for all $r > 1/\sqrt{N-1}$, which is due to the underlying assumption that $\mathcal{T}' \in \text{MVES}(\mathcal{R}(r))$ for $1/\sqrt{N-1} < r \leq 1$. Consider the following lemma:

Lemma 4 *Suppose that $\mathcal{W}, \mathcal{W}' \in \text{MVES}(\mathcal{B}(r))$, where $\mathcal{B}(r)$ is defined in (37). Also, suppose that $\mathcal{R} = \mathcal{W} \cap \mathcal{B}(\bar{r}) \subseteq \mathcal{W}'$ for some $\bar{r} > r > 0$. Then we have $\mathcal{W} = \mathcal{W}'$.*

The proof of Lemma 4 is relegated to Appendix C. By Lemma 4, we obtain $\mathcal{W}_e = \mathcal{W}'$, and consequently, $\mathcal{T}_e = \mathcal{T}'$.

E. Proof of Proposition 2

Assume $N = 2$, and let $\text{conv}\{\mathbf{b}_1, \mathbf{b}_2\}$ be an MVES of \mathcal{S}_L , where $\mathbf{b}_1, \mathbf{b}_2 \in \text{aff}\{\mathbf{e}_1, \mathbf{e}_2\} \subseteq \mathbb{R}^2$. Using the simple fact $\text{aff}\{\mathbf{e}_1, \mathbf{e}_2\} = \{\mathbf{s} \in \mathbb{R}^2 \mid s_1 + s_2 = 1\}$, we can write

$$\mathbf{b}_1 = \begin{bmatrix} \beta_1 \\ 1 - \beta_1 \end{bmatrix}, \mathbf{b}_2 = \begin{bmatrix} \beta_2 \\ 1 - \beta_2 \end{bmatrix},$$

for some coefficients $\beta_1, \beta_2 \in \mathbb{R}$. By the same spirit, every abundance vector \mathbf{s}_n (for $N = 2$) can be written as

$$\mathbf{s}_n = \begin{bmatrix} \alpha_n \\ 1 - \alpha_n \end{bmatrix}, \quad n = 1, \dots, L,$$

where $0 \leq \alpha_n \leq 1$. From the above expressions, it is easy to show that the MVES enclosing property $\mathbf{s}_n \in \text{conv}\{\mathbf{b}_1, \mathbf{b}_2\}$ is equivalent to

$$\beta_2 \leq \alpha_n \leq \beta_1, \quad n = 1, \dots, L, \quad (39)$$

where we assume $\beta_1 \geq \beta_2$ w.l.o.g. Moreover, from the simplex volume formula in (1), the volume of $\text{conv}\{\mathbf{b}_1, \mathbf{b}_2\}$ is

$$\text{vol}(\text{conv}\{\mathbf{b}_1, \mathbf{b}_2\}) = \beta_1 - \beta_2. \quad (40)$$

From (39)-(40), it is immediate that $\text{conv}\{\mathbf{b}_1, \mathbf{b}_2\}$ is a minimum volume simplex enclosing \mathcal{S}_L if and only if

$$\beta_2 = \min_{n=1, \dots, L} \alpha_n, \quad \beta_1 = \max_{n=1, \dots, L} \alpha_n. \quad (41)$$

Now, consider perfect identifiability $\{\mathbf{b}_1, \mathbf{b}_2\} = \{\mathbf{e}_1, \mathbf{e}_2\}$, which is equivalent to $\beta_1 = 1, \beta_2 = 0$. Putting the above conditions into (41), we see that perfect identifiability is achieved if and only if the pure-pixel assumption holds; i.e., there exist two pixels, indexed by n_1 and n_2 , such that $\mathbf{s}_{n_1} = \mathbf{e}_1$ and $\mathbf{s}_{n_2} = \mathbf{e}_2$ (or $\alpha_{n_1} = 1, \alpha_{n_2} = 0$), resp.

F. Proof of Theorem 4

Let

$$\mathbf{p}_{ij} = \alpha \mathbf{e}_i + (1 - \alpha) \mathbf{e}_j, \quad (42)$$

for $i, j \in \{1, \dots, N\}, i \neq j$, and recall $\alpha = \min_{i \neq j} \alpha_{ij}$. It can be verified that each \mathbf{p}_{ij} is a convex combination of $\mathbf{s}_{n(i,j)}$ and $\mathbf{s}_{n(j,i)}$ in (7). Thus, every \mathbf{p}_{ij} satisfies $\mathbf{p}_{ij} \in \text{conv}\mathcal{S}_L$. For notational convenience, let

$$\mathcal{P} = \{\mathbf{p}_{ij}\}_{i,j \in \{1, \dots, N\}, i \neq j}$$

denote the set that collects all the \mathbf{p}_{ij} 's. By the result $\mathbf{p}_{ij} \in \text{conv}\mathcal{S}_L$, we have $\text{conv}\mathcal{P} \subseteq \text{conv}\mathcal{S}_L$, and consequently,

$$\mathcal{R}(r) \subseteq \text{conv}\mathcal{S}_L \iff \mathcal{R}(r) \subseteq \text{conv}\mathcal{P}.$$

Applying the above implication to γ in (5) yields

$$\gamma \geq \sup\{r \leq 1 \mid \mathcal{R}(r) \subseteq \text{conv}\mathcal{P}\} \quad (43)$$

Eq. (43) has an explicit expression. To show it, let us first consider the following lemma.

Lemma 5 *For any $\alpha \in (0.5, 1]$, $\text{conv}\mathcal{P}$ is equivalent to*

$$\text{conv}\mathcal{P} = \{\mathbf{s} \in \mathcal{T}_e \mid s_i \leq \alpha, i = 1, \dots, N\}. \quad (44)$$

The proof of Lemma 5 is relegated to Appendix E. By using Lemma 5, and observing the expressions of $\mathcal{R}(r)$ in (5) and $\text{conv}\mathcal{P}$ in (44), we see the following equivalence

$$\begin{aligned} \mathcal{R}(r) \subseteq \text{conv}\mathcal{P} &\iff \max_{i=1, \dots, N} s_i \leq \alpha \text{ for all } \mathbf{s} \in \mathcal{R}(r) \\ &\iff \sup_{\mathbf{s} \in \mathcal{R}(r)} \max_{i=1, \dots, N} s_i \leq \alpha, \end{aligned} \quad (45)$$

for $\frac{1}{\sqrt{N}} \leq r \leq 1$ (note that $\mathcal{R}(r) = \emptyset$ for $r < \frac{1}{\sqrt{N}}$). Next, we solve the maximization problem in (45). The result is summarized in the following lemma.

Lemma 6 *Let*

$$\alpha^*(r) = \sup_{\mathbf{s} \in \mathcal{R}(r)} \max_{i=1, \dots, N} s_i,$$

where $N \geq 2$ and $\frac{1}{\sqrt{N}} \leq r \leq 1$. The optimal value $\alpha^*(r)$ has a closed-form expression

$$\alpha^*(r) = \frac{1 + \sqrt{(N-1)(Nr^2 - 1)}}{N}.$$

The proof of Lemma 6 is shown in Appendix F. Now, by applying Lemma 6 and (45) to (43), we get

$$\gamma \geq \sup\{r \in [1/\sqrt{N}, 1] \mid \alpha^*(r) \leq \alpha\}. \quad (46)$$

By noting that $\alpha^*(r)$ is an increasing function of $r \in [1/\sqrt{N}, 1]$, we see that if there exists an $r \in [1/\sqrt{N}, 1]$ such that $\alpha^*(r) = \alpha$, then that r attains the supremum in (46). It can be verified that the solution to $\alpha^*(r) = \alpha$ is

$$r = \sqrt{\frac{1}{N} \left[\frac{(N\alpha - 1)^2}{N - 1} + 1 \right]},$$

and the above r satisfies $r \in [1/\sqrt{N}, 1]$ for $0.5 < \alpha \leq 1$, $N \geq 2$. Putting the above solution into (46), we obtain the desired result in Theorem 4.

V. NUMERICAL EXPERIMENTS

In this section, we provide numerical simulation results that aim to support the theoretical MVES identifiability results proven in the previous section. The signals are generated by the following way. The observed data set $\{\mathbf{x}_1, \dots, \mathbf{x}_L\}$ follows the basic model in (2). The endmember signature vectors $\mathbf{a}_1, \dots, \mathbf{a}_N$ are selected from the U.S. geological survey (USGS) library [28], and the number of spectral bands is $M = 224$. The generation of the abundance vectors is similar to that in [6]. Specifically, we generate a large pool of random vectors following a Dirichlet distribution with parameter $\boldsymbol{\mu} = \frac{1}{N}\mathbf{1}$, and then select a number of L such random vectors as the abundance set $\{s_1, \dots, s_L\}$. During the selection, we do not choose vectors whose 2-norm exceeds a given parameter r ; the reason of doing so is to allow us to control the pixel purity level of $\{s_1, \dots, s_L\}$ at or below r in the simulations. Note that if the number of pixels L is large, then one should expect that r be close to the best pixel purity level ρ and uniform pixel purity level γ . In the simulations, we set $L = 1,000$.

The simulation settings are as follows. MVES is implemented by the alternating linear programming method in [6]. We measure its identification performance by using the root-mean-square (RMS) angle error

$$\phi = \min_{\pi \in \Pi_N} \sqrt{\frac{1}{N} \sum_{i=1}^N \left[\arccos \left(\frac{\mathbf{a}_i^T \hat{\mathbf{a}}_{\pi_i}}{\|\mathbf{a}_i\| \cdot \|\hat{\mathbf{a}}_{\pi_i}\|} \right) \right]^2},$$

where $\{\hat{\mathbf{a}}_1, \dots, \hat{\mathbf{a}}_N\}$ denotes the MVES estimate of the endmembers, and Π_N denotes the set of all permutations of $\{1, \dots, N\}$. A number of 50 randomly generated realizations were run to evaluate the means and standard deviations of ϕ .

The obtained RMS angle error results are shown in Figure 5. We see that zero RMS angle error, or equivalently, perfect identifiability, is attained when $r > 1/\sqrt{N-1}$ — which is a good match with the sufficient MVES identifiability result in Theorem 2. Also, we observe non-zero errors for $r \leq 1/\sqrt{N-1}$, which matches the necessary MVES identifiability result in Theorem 1.

Before closing this experiment section, we should mention that previous papers, such as [6], [15], [17]–[21], have together provided a nice and rather complete coverage on MVES's performance under both synthetic and real-data experiments. Hence, readers are referred to such papers for more experimental results. The results reported therein also indicate that MVES-based algorithms are robust against lack of pure pixels.

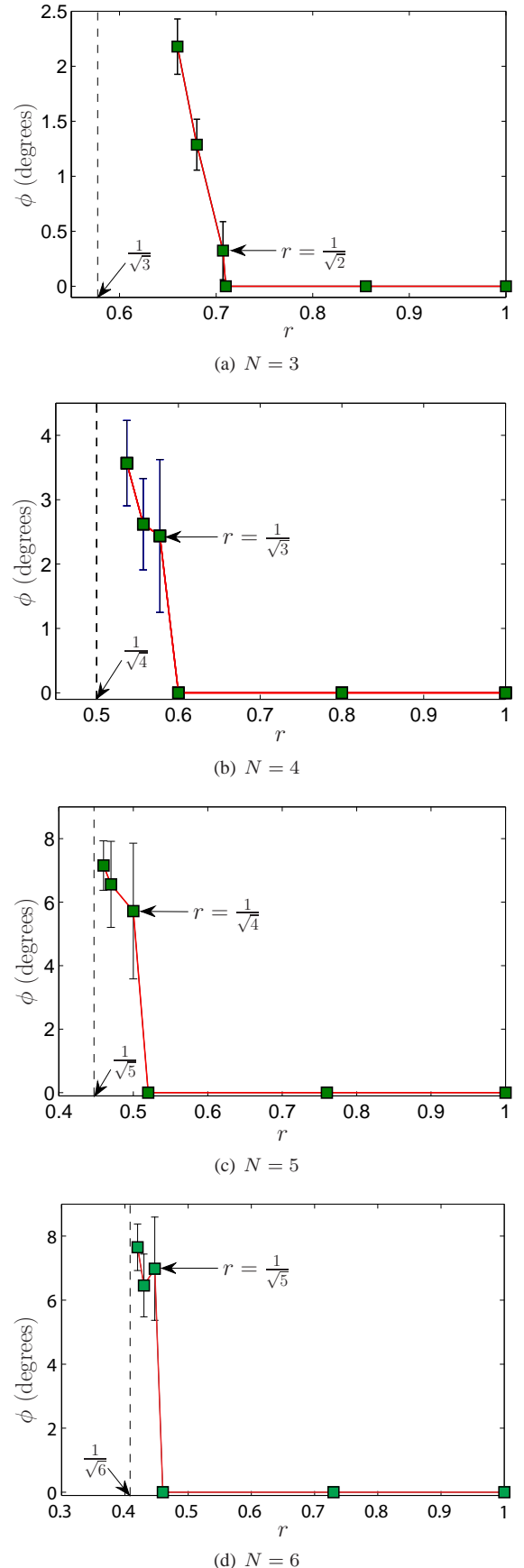


Fig. 5. MVES performance with respect to the numerically control pixel purity level r .

The numerical (and also theoretical) results above further show the limit of robustness— $1/\sqrt{N-1}$ with the uniform pixel purity level.

VI. CONCLUSION

In this paper, a theoretical analysis for the identifiability of MVES in blind HU was performed. The results suggest that under some mild assumptions which are considerably more relaxed than those for the pure-pixel case, MVES exhibits robustness against lack of pure pixels. Hence, our study provides a theoretical explanation on why numerical studies usually found that MVES can recover the endmembers accurately in the no pure-pixel case.

ACKNOWLEDGEMENT

The authors would like to thank the anonymous reviewers and associate editor, who have helped us improve the paper significantly.

APPENDIX

A. Proof of Lemma 1

Let us first prove Lemma 1.(a). The set \mathcal{T}_G can be explicitly represented by

$$\mathcal{T}_G = \text{conv}\{\mathbf{g}_1, \dots, \mathbf{g}_N\},$$

where $\mathbf{g}_i \in \mathbb{R}^N$ for all i . Also, by letting $\mathbf{h}_i = \mathbf{A}\mathbf{g}_i$ for all i , one can easily show that

$$f(\mathcal{T}_G) = \text{conv}\{\mathbf{h}_1, \dots, \mathbf{h}_N\}.$$

Since $\mathcal{T}_G \subset \text{aff}\{\mathbf{e}_1, \dots, \mathbf{e}_N\}$, we have $\mathbf{g}_i \in \text{aff}\{\mathbf{e}_1, \dots, \mathbf{e}_N\}$ for all i . This means that each \mathbf{g}_i satisfies $\mathbf{1}^T \mathbf{g}_i = 1$, or equivalently, $g_{i,N} = 1 - \sum_{j=1}^{N-1} g_{i,j}$. Using the above fact, we can write

$$\mathbf{g}_i = \mathbf{C}\boldsymbol{\theta}_i + \mathbf{e}_N,$$

where $\boldsymbol{\theta}_i = [\mathbf{g}_i]_{1:(N-1)}$, and

$$\mathbf{C} = \begin{bmatrix} \mathbf{I} \\ -\mathbf{1}^T \end{bmatrix} \in \mathbb{R}^{N \times (N-1)}.$$

Let $\bar{\mathbf{G}} = [\mathbf{g}_1 - \mathbf{g}_N, \dots, \mathbf{g}_{N-1} - \mathbf{g}_N]$. We get

$$\bar{\mathbf{G}} = \mathbf{C}\bar{\boldsymbol{\Theta}},$$

where $\bar{\boldsymbol{\Theta}} = [\boldsymbol{\theta}_1 - \boldsymbol{\theta}_N, \dots, \boldsymbol{\theta}_{N-1} - \boldsymbol{\theta}_N] \in \mathbb{R}^{(N-1) \times (N-1)}$. We therefore obtain

$$\det(\bar{\mathbf{G}}^T \bar{\mathbf{G}}) = \det(\bar{\boldsymbol{\Theta}}^T \mathbf{C}^T \mathbf{C} \bar{\boldsymbol{\Theta}}) \quad (47a)$$

$$= \det(\bar{\boldsymbol{\Theta}}) \det(\mathbf{C}^T \mathbf{C}) \det(\bar{\boldsymbol{\Theta}}) \quad (47b)$$

$$= N \cdot |\det(\bar{\boldsymbol{\Theta}})|^2, \quad (47c)$$

where (47b) is due to $\det(\mathbf{AB}) = \det(\mathbf{A})\det(\mathbf{B})$ for square \mathbf{A}, \mathbf{B} , and (47c) is due to the following result

$$\det(\mathbf{C}^T \mathbf{C}) = \det(\mathbf{I} + \mathbf{1}\mathbf{1}^T) = N$$

(note that the matrix result $\det(\mathbf{I} + \mathbf{q}\mathbf{q}^T) = \|\mathbf{q}\|^2 + 1$ has been used). Likewise, by letting $\bar{\mathbf{H}} = [\mathbf{h}_1 - \mathbf{h}_N, \dots, \mathbf{h}_{N-1} - \mathbf{h}_N]$, we have

$$\bar{\mathbf{H}} = \mathbf{A}\bar{\mathbf{G}} = \mathbf{A}\mathbf{C}\bar{\boldsymbol{\Theta}} = \bar{\mathbf{A}}\bar{\boldsymbol{\Theta}},$$

and

$$\det(\bar{\mathbf{H}}^T \bar{\mathbf{H}}) = \det(\bar{\mathbf{A}}^T \bar{\mathbf{A}}) \cdot |\det(\bar{\boldsymbol{\Theta}})|^2. \quad (48)$$

Now, by (1), (47) and (48), Eq. (8) is obtained. Also, the property $f(\mathcal{T}_G) \subset \text{aff}\{\mathbf{a}_1, \dots, \mathbf{a}_N\}$ can be easily proven by the fact that $\bar{\mathbf{H}} = \mathbf{A}\bar{\mathbf{G}}$ and $\mathbf{1}^T \mathbf{g}_i = 1$ for all i .

Next, we prove Lemma 1.(b). The set \mathcal{T}_H can be written as

$$\mathcal{T}_H = \text{conv}\{\mathbf{h}_1, \dots, \mathbf{h}_N\},$$

where $\mathbf{h}_i \in \mathbb{R}^M$ for all i . Since $\mathcal{T}_H \subset \text{aff}\{\mathbf{a}_1, \dots, \mathbf{a}_N\}$, we have $\mathbf{h}_i \in \text{aff}\{\mathbf{a}_1, \dots, \mathbf{a}_N\}$ for all i . Hence, each \mathbf{h}_i can be expressed as $\mathbf{h}_i = \mathbf{A}\mathbf{g}_i$, where $\mathbf{g}_i \in \mathbb{R}^N$, $\mathbf{1}^T \mathbf{g}_i = 1$. This leads to

$$f^{-1}(\mathcal{T}_H) = \{ \mathbf{x} \mid \mathbf{A}\mathbf{x} \in \text{conv}\{\mathbf{h}_1, \dots, \mathbf{h}_N\} \} \quad (49a)$$

$$= \{ \mathbf{x} \mid \mathbf{A}\mathbf{x} = \mathbf{H}\boldsymbol{\theta}, \boldsymbol{\theta} \geq \mathbf{0}, \mathbf{1}^T \boldsymbol{\theta} = 1 \} \quad (49b)$$

$$= \{ \mathbf{x} \mid \mathbf{A}\mathbf{x} = \mathbf{A}\mathbf{G}\boldsymbol{\theta}, \boldsymbol{\theta} \geq \mathbf{0}, \mathbf{1}^T \boldsymbol{\theta} = 1 \} \quad (49c)$$

$$= \{ \mathbf{x} \mid \mathbf{x} = \mathbf{G}\boldsymbol{\theta}, \boldsymbol{\theta} \geq \mathbf{0}, \mathbf{1}^T \boldsymbol{\theta} = 1 \} \quad (49d)$$

$$= \text{conv}\{\mathbf{g}_1, \dots, \mathbf{g}_N\} \quad (49e)$$

$$\subset \text{aff}\{\mathbf{e}_1, \dots, \mathbf{e}_N\}, \quad (49f)$$

where (49d) is due to the full column rank condition of \mathbf{A} , and (49f) uses the structure $\mathbf{1}^T \mathbf{g}_i = 1$. The rest of the proof is the same as that of Lemma 1.(a).

B. Proof of Lemma 3

Fix $r = 1/\sqrt{N-1}$. From (22), $\mathcal{C}(r)$ can be re-expressed as

$$\mathcal{C}(r) = \{ \mathbf{s} = \mathbf{C}\boldsymbol{\theta} + \mathbf{d} \mid \boldsymbol{\theta} \in \mathcal{B}(\mu) \}, \quad (50)$$

where $\mu = \sqrt{r^2 - 1/N} = 1/\sqrt{(N-1)N}$, and

$$\mathcal{B}(r') = \{ \boldsymbol{\theta} \in \mathbb{R}^{N-1} \mid \|\boldsymbol{\theta}\| \leq r' \} \quad (51)$$

is a ball on \mathbb{R}^{N-1} . Also, recall from (17)-(18) that an MVES $\mathcal{V} \in \text{MVES}(\mathcal{C}(r))$ can be written as

$$\mathcal{V} = \{ \mathbf{s} = \mathbf{C}\boldsymbol{\theta} + \mathbf{d} \mid \boldsymbol{\theta} \in \mathcal{W} \}, \quad (52)$$

where $\mathcal{W} = \text{conv}\{\mathbf{w}_1, \dots, \mathbf{w}_N\} \subseteq \mathbb{R}^{N-1}$; and that $\text{vol}(\mathcal{V}) = \text{vol}(\mathcal{W})$ (see (19)). From the expressions above, we can deduce the following result: \mathcal{W} must be an MVES of $\mathcal{B}(\mu)$ if \mathcal{V} is an MVES of $\mathcal{C}(r)$, and the converse is also true.

Next, we will use the following fact:

Fact 2 [29, Theorem 3.2] *The volume of an $(N-1)$ -dimensional simplex \mathcal{W} enclosing $B(r')$ in (51) satisfies*

$$\text{vol}(\mathcal{W}) \geq \frac{1}{(N-1)!} N^{\frac{N}{2}} (N-1)^{\frac{1}{2}(N-1)} (r')^{N-1} \quad (53)$$

with equality only for the regular simplex.

Using Fact 2 and the result $\text{vol}(\mathcal{V}) = \text{vol}(\mathcal{W})$, we obtain

$$\text{vol}(\mathcal{V}) = \frac{1}{(N-1)!} \sqrt{N},$$

where we should note that the right-hand side of the above equation is obtained by putting $r' = \mu = 1/\sqrt{(N-1)N}$ into (53). On the other hand, consider $\mathcal{T}_e = \text{conv}\{\mathbf{e}_1, \dots, \mathbf{e}_N\}$,

which encloses $\mathcal{C}(r)$ (for $r = 1/\sqrt{N-1}$). From the simplex volume formula (1), one can show that

$$\text{vol}(\mathcal{T}_e) = \frac{1}{(N-1)!} \sqrt{N}.$$

Since \mathcal{T}_e attains the same volume as \mathcal{V} , \mathcal{T}_e is an MVES of $\mathcal{C}(r)$.

C. Proof of Lemma 4

The following lemma will be required:

Lemma 7 Let $\mathcal{B}(r) = \{\boldsymbol{\theta} \in \mathbb{R}^{N-1} \mid \|\boldsymbol{\theta}\| \leq r\}$, where $r > 0$. For any $\mathcal{W} \in \text{MVES}(\mathcal{B}(r))$, the boundaries of $\mathcal{B}(r)$ and \mathcal{W} have exactly N intersecting points. Also, by letting $\{\mathbf{t}_1, \dots, \mathbf{t}_N\} = \text{bd}\mathcal{B}(r) \cap \text{bd}\mathcal{W}$ be the set of those intersecting points, we have the following properties:

- (a) The points $\mathbf{t}_1, \dots, \mathbf{t}_N$ are affinely independent.
- (b) The simplex \mathcal{W} can be constructed from $\mathbf{t}_1, \dots, \mathbf{t}_N$ via

$$\mathcal{W} = \bigcap_{i=1}^N \{\boldsymbol{\theta} \in \mathbb{R}^{N-1} \mid r^2 \geq \mathbf{t}_i^T \boldsymbol{\theta}\}.$$

The proof of Lemma 7 is given in Appendix D. Let

$$\begin{aligned} \{\mathbf{t}_1, \dots, \mathbf{t}_N\} &= \text{bd}\mathcal{B}(r) \cap \text{bd}\mathcal{W}, \\ \{\mathbf{t}'_1, \dots, \mathbf{t}'_N\} &= \text{bd}\mathcal{B}(r) \cap \text{bd}\mathcal{W}', \end{aligned}$$

which, by Lemma 7, always exist. Since $\mathcal{B}(r) \subset \mathcal{W}$ and $\mathcal{B}(r) \subset \mathcal{W}'$, the above two equations can be equivalently expressed as

$$\{\mathbf{t}_1, \dots, \mathbf{t}_N\} = \text{bd}\mathcal{B}(r) \setminus \text{int}\mathcal{W}, \quad (54)$$

$$\{\mathbf{t}'_1, \dots, \mathbf{t}'_N\} = \text{bd}\mathcal{B}(r) \setminus \text{int}\mathcal{W}'. \quad (55)$$

Also, by Lemma 7.(b), we have $\mathcal{W} = \mathcal{W}'$ if $\{\mathbf{t}_1, \dots, \mathbf{t}_N\} = \{\mathbf{t}'_1, \dots, \mathbf{t}'_N\}$. In the following steps we focus on proving $\{\mathbf{t}_1, \dots, \mathbf{t}_N\} = \{\mathbf{t}'_1, \dots, \mathbf{t}'_N\}$.

Step 1: We first prove

$$\text{bd}(\mathcal{W} \cap \mathcal{B}(\bar{r})) \subseteq \text{bd}\mathcal{W} \cup \text{bd}\mathcal{B}(\bar{r}) \quad (56)$$

by contradiction. Suppose that (56) does not hold, namely, there exists an $\mathbf{x} \in \mathbb{R}^{N-1}$ satisfying

$$\mathbf{x} \in \text{bd}(\mathcal{W} \cap \mathcal{B}(\bar{r})), \text{ but} \quad (57)$$

$$\mathbf{x} \notin \text{bd}\mathcal{W} \cup \text{bd}\mathcal{B}(\bar{r}). \quad (58)$$

Now, since $\mathcal{W} \cap \mathcal{B}(\bar{r})$ is a closed set, (57) implies

$$\mathbf{x} \in \mathcal{W} \cap \mathcal{B}(\bar{r}). \quad (59)$$

Equations (58) and (59) imply that $\mathbf{x} \in \text{int}\mathcal{W}$ and that $\mathbf{x} \in \text{int}\mathcal{B}(\bar{r})$. Thus, we have $\mathbf{x} \in \text{int}(\mathcal{W} \cap \mathcal{B}(\bar{r}))$ which contradicts (57). Hence, (56) must hold.

Step 2: We show that $\{\mathbf{t}_1, \dots, \mathbf{t}_N\} = \text{bd}\mathcal{B}(r) \cap \text{bd}\mathcal{R}$. Let us first consider proving $\{\mathbf{t}_1, \dots, \mathbf{t}_N\} \subseteq \text{bd}\mathcal{B}(r) \cap \text{bd}\mathcal{R}$. We observe from $\mathcal{B}(r) \subseteq \mathcal{B}(\bar{r})$ and $\mathcal{B}(r) \subseteq \mathcal{W}$ that

$$\mathcal{B}(r) \subseteq \mathcal{B}(\bar{r}) \cap \mathcal{W} = \mathcal{R}. \quad (60)$$

Subsequently, the following inequality chain can be derived:

$$\{\mathbf{t}_1, \dots, \mathbf{t}_N\} = \text{bd}\mathcal{B}(r) \setminus \text{int}\mathcal{W} \quad (61a)$$

$$\subseteq \text{bd}\mathcal{B}(r) \setminus (\text{int}\mathcal{W} \cap \text{int}\mathcal{B}(\bar{r})) \quad (61b)$$

$$= \text{bd}\mathcal{B}(r) \setminus \text{int}\mathcal{R} \quad (61c)$$

$$= \text{bd}\mathcal{B}(r) \cap \text{bd}\mathcal{R}, \quad (61d)$$

where (61a) is by (54); (61c) is by $\text{int}(\mathcal{W} \cap \mathcal{B}(\bar{r})) = \text{int}\mathcal{W} \cap \text{int}\mathcal{B}(\bar{r})$; (61d) is by (60).

Moreover, we have $\text{bd}\mathcal{B}(r) \cap \text{bd}\mathcal{R} \subseteq \{\mathbf{t}_1, \dots, \mathbf{t}_N\}$, obtained from the following chain:

$$\text{bd}\mathcal{B}(r) \cap \text{bd}\mathcal{R} = \text{bd}\mathcal{B}(r) \cap \text{bd}(\mathcal{W} \cap \mathcal{B}(\bar{r})) \quad (62a)$$

$$\subseteq \text{bd}\mathcal{B}(r) \cap (\text{bd}\mathcal{W} \cup \text{bd}\mathcal{B}(\bar{r})) \quad (62b)$$

$$= (\text{bd}\mathcal{B}(r) \cap \text{bd}\mathcal{W}) \cup (\text{bd}\mathcal{B}(r) \cap \text{bd}\mathcal{B}(\bar{r})) \quad (62c)$$

$$= (\text{bd}\mathcal{B}(r) \cap \text{bd}\mathcal{W}) \cup \emptyset \quad (62d)$$

$$= \text{bd}\mathcal{B}(r) \setminus \text{int}\mathcal{W} \quad (62e)$$

$$= \{\mathbf{t}_1, \dots, \mathbf{t}_N\}, \quad (62f)$$

where (62b) is by (56); (62d) is by $\bar{r} > r$; (62e) is by $\text{bd}\mathcal{B}(r) \subseteq \mathcal{B}(r) \subseteq \mathcal{W}$; (62f) is by (54).

Step 3: We prove $\{\mathbf{t}_1, \dots, \mathbf{t}_N\} = \{\mathbf{t}'_1, \dots, \mathbf{t}'_N\}$. In Step 2, it is shown that

$$\{\mathbf{t}_1, \dots, \mathbf{t}_N\} = \text{bd}\mathcal{B}(r) \cap \text{bd}\mathcal{R}. \quad (63)$$

By the fact that $\mathbf{t}'_i \in \mathcal{B}(r)$ and by (60), we have

$$\mathbf{t}'_i \in \mathcal{R}. \quad (64)$$

Moreover, from the assumption that $\mathcal{R} \subseteq \mathcal{W}'$, we have $\text{bd}\mathcal{W}' \cap \text{int}\mathcal{R} = \emptyset$. But from (55), we note that $\mathbf{t}'_i \in \text{bd}\mathcal{W}'$. Thus we can conclude $\mathbf{t}'_i \notin \text{int}(\mathcal{R})$, which together with (64) yields

$$\mathbf{t}'_i \in \text{bd}\mathcal{R}. \quad (65)$$

Combining $\mathbf{t}'_i \in \text{bd}\mathcal{B}(r)$ (cf. (55)) with (63) and (65), we obtain $\mathbf{t}'_i \in \{\mathbf{t}_1, \dots, \mathbf{t}_N\}$. Since Property (a) in Lemma 7 restricts $\mathbf{t}'_1, \dots, \mathbf{t}'_N$ to be affinely independent, the only possible choice of $\mathbf{t}'_1, \dots, \mathbf{t}'_N$ is $\{\mathbf{t}'_1, \dots, \mathbf{t}'_N\} = \{\mathbf{t}_1, \dots, \mathbf{t}_N\}$. Lemma 4 is therefore proven.

D. Proof of Lemma 7

The proof of Lemma 7 requires several convex analysis results. To start with, consider the following results:

Fact 3 Let $\mathcal{W} = \text{conv}\{\mathbf{w}_1, \dots, \mathbf{w}_N\} \subset \mathbb{R}^{N-1}$ denote an $(N-1)$ -dimensional simplex. Also, let

$$\begin{aligned} \mathcal{P}(\mathbf{g}, \mathbf{H}) &= \{\boldsymbol{\theta} \in \mathbb{R}^{N-1} \mid \mathbf{H}^T \boldsymbol{\theta} + \mathbf{g} \geq \mathbf{0}, \\ &\quad -(\mathbf{H}\mathbf{1})^T \boldsymbol{\theta} + (1 - \mathbf{1}^T \mathbf{g}) \geq 0\} \end{aligned} \quad (66)$$

denote a polyhedron, where $(\mathbf{g}, \mathbf{H}) \in \mathbb{R}^{N-1} \times \mathbb{R}^{(N-1) \times (N-1)}$ is given.

- (a) Any \mathcal{W} can be equivalently represented by $\mathcal{P}(\mathbf{g}, \mathbf{H})$ via setting

$$\mathbf{H} = \bar{\mathbf{W}}^{-T}, \quad \mathbf{g} = -\bar{\mathbf{W}}^{-T} \mathbf{w}_N, \quad (67)$$

where $\bar{\mathbf{W}} = [\mathbf{w}_1 - \mathbf{w}_N, \dots, \mathbf{w}_{N-1} - \mathbf{w}_N]$.

- (b) Suppose that \mathbf{H} has full rank. Under the above restriction, the set $\mathcal{P}(\mathbf{g}, \mathbf{H})$ for any (\mathbf{g}, \mathbf{H}) can be equivalently represented by \mathcal{W} , whose vertices $\mathbf{w}_1, \dots, \mathbf{w}_N$ can be determined by solving the inverse of (67). Also, the corresponding volume is

$$\text{vol}(\mathcal{P}(\mathbf{g}, \mathbf{H})) = \frac{1}{(N-1)!} |\det(\mathbf{H})|^{-1}. \quad (68)$$

The proof of Fact 3 has been shown in the literature [6], [23]. Also, (68) is determined by the simplex volume formula (1) and the relation in (67). From Fact 3, we derive several convex analysis properties for proving Lemma 7.

Fact 4 Let \mathcal{W} be an $(N-1)$ -dimensional simplex on \mathbb{R}^{N-1} , and consider the polyhedral representation of \mathcal{W} in (66)-(67). Also, recall the definition $\mathcal{B}(r) = \{\boldsymbol{\theta} \in \mathbb{R}^{N-1} \mid \|\boldsymbol{\theta}\| \leq r\}$.

- (a) If $\mathcal{B}(r) \subseteq \mathcal{W}$, then the following equations hold

$$-r\|\mathbf{h}_i\| + g_i \geq 0, \quad i = 1, \dots, N-1, \quad (69a)$$

$$-r\|\mathbf{H}\mathbf{1}\| + (1 - \mathbf{1}^T \mathbf{g}) \geq 0, \quad (69b)$$

where \mathbf{h}_i and g_i denote the i th column of \mathbf{H} and i th element of \mathbf{g} , resp. Conversely, if (69) holds, then $\mathcal{B}(r) \subseteq \mathcal{W}$.

- (b) Suppose $\mathcal{B}(r) \subseteq \mathcal{W}$. The boundaries of $\mathcal{B}(r)$ and \mathcal{W} have at most N intersecting points. Specifically, we have $\text{bd}\mathcal{B}(r) \cap \text{bd}\mathcal{W} \subseteq \{\mathbf{t}_1, \dots, \mathbf{t}_N\}$ where

$$\mathbf{t}_i = -\frac{r}{\|\mathbf{h}_i\|} \mathbf{h}_i, \quad i = 1, \dots, N-1, \quad (70a)$$

$$\mathbf{t}_N = \frac{r}{\|\mathbf{H}\mathbf{1}\|} \mathbf{H}\mathbf{1}. \quad (70b)$$

Also, if $\mathbf{t}_i \in \text{bd}\mathcal{B}(r) \cap \text{bd}\mathcal{W}$, then

$$\begin{cases} -r\|\mathbf{h}_i\| + g_i = 0, & i \in \{1, \dots, N-1\}, \\ -r\|\mathbf{H}\mathbf{1}\| + (1 - \mathbf{1}^T \mathbf{g}) = 0, & i = N; \end{cases} \quad (71)$$

otherwise

$$\begin{cases} -r\|\mathbf{h}_i\| + g_i > 0, & i \in \{1, \dots, N-1\}, \\ -r\|\mathbf{H}\mathbf{1}\| + (1 - \mathbf{1}^T \mathbf{g}) > 0, & i = N. \end{cases} \quad (72)$$

Proof of Fact 4: The proof of Fact 4.(a) basically follows the development in [23, pp.148-149], and is omitted here for conciseness. To prove Fact 4.(b), observe that a point $\tilde{\boldsymbol{\theta}} \in \text{bd}\mathcal{B}(r) \cap \text{bd}\mathcal{W}$ satisfies i) $\|\tilde{\boldsymbol{\theta}}\| = r$; and ii) either

$$\mathbf{h}_i^T \tilde{\boldsymbol{\theta}} + g_i = 0, \quad (73)$$

for some $i \in \{1, \dots, N-1\}$, or

$$-(\mathbf{H}\mathbf{1})^T \tilde{\boldsymbol{\theta}} + (1 - \mathbf{1}^T \mathbf{g}) = 0. \quad (74)$$

Suppose that $\tilde{\boldsymbol{\theta}}$ satisfies (73). Recall that the assumption $\mathcal{B}(r) \subseteq \mathcal{W}$ implies

$$\mathbf{h}_i^T \boldsymbol{\theta} + g_i \geq 0, \quad \text{for all } \|\boldsymbol{\theta}\| \leq r, \quad (75)$$

and that the left-hand side of (75) attains its minimum if and only if $\boldsymbol{\theta} = -(r/\|\mathbf{h}_i\|)\mathbf{h}_i = \mathbf{t}_i$. Thus, if (73) is to be satisfied, then $\tilde{\boldsymbol{\theta}}$ must equal \mathbf{t}_i , and subsequently (73) becomes

$$-r\|\mathbf{h}_i\| + g_i = 0. \quad (76)$$

Likewise, it is shown that if $\tilde{\boldsymbol{\theta}}$ satisfies (74), then $\tilde{\boldsymbol{\theta}} = (r/\|\mathbf{H}\mathbf{1}\|)\mathbf{H}\mathbf{1} = \mathbf{t}_N$ is the only choice and (74) becomes

$$-r\|\mathbf{H}\mathbf{1}\| + (1 - \mathbf{1}^T \mathbf{g}) = 0. \quad (77)$$

We therefore complete the proof that $\tilde{\boldsymbol{\theta}} \in \text{bd}\mathcal{B}(r) \cap \text{bd}\mathcal{W}$ implies $\tilde{\boldsymbol{\theta}} \in \{\mathbf{t}_1, \dots, \mathbf{t}_N\}$.

We should also mention (71)-(72). From the proof above, it is clear that $\mathbf{t}_i \in \text{bd}\mathcal{B}(r) \cap \text{bd}\mathcal{W}$ holds if and only if (76) holds for $i = 1, \dots, N-1$, and (77) holds for $i = N$, respectively. By considering (69) as well, we obtain the conditions in (71)-(72). ■

We are now ready to prove Lemma 7. Recall that $\mathcal{W} \in \text{MVES}(\mathcal{B}(r))$ is assumed. By Fact 3.(a), we can write $\mathcal{W} = \mathcal{P}(\mathbf{g}, \mathbf{H})$ for some (\mathbf{g}, \mathbf{H}) , with \mathbf{H} being of full rank. Then, by Fact 4.(b), we obtain $\text{bd}\mathcal{B}(r) \cap \text{bd}\mathcal{W} \subseteq \{\mathbf{t}_1, \dots, \mathbf{t}_N\}$. We consider two cases.

Case 1: Suppose that $\mathbf{t}_i \notin \text{bd}\mathcal{B}(r) \cap \text{bd}\mathcal{W}$ for some $i \in \{1, \dots, N-1\}$. For simplicity but w.l.o.g., assume $i = 1$. By Fact 4.(a)-(b), we have

$$-r\|\mathbf{h}_1\| + g_1 > 0, \quad (78a)$$

$$-r\|\mathbf{h}_i\| + g_i \geq 0, \quad i = 2, \dots, N-1, \quad (78b)$$

$$-r\|\mathbf{H}\mathbf{1}\| + (1 - \mathbf{1}^T \mathbf{g}) \geq 0. \quad (78c)$$

Let us construct another polyhedron, denoted by $\mathcal{P}(\tilde{\mathbf{g}}, \tilde{\mathbf{H}})$, where the 2-tuple $(\tilde{\mathbf{g}}, \tilde{\mathbf{H}}) \in \mathbb{R}^{N-1} \times \mathbb{R}^{(N-1) \times (N-1)}$ is chosen as

$$\tilde{g}_1 = g_1 - N\epsilon, \quad (79a)$$

$$\tilde{g}_i = g_i + \epsilon, \quad i = 2, \dots, N-1, \quad (79b)$$

$$\tilde{\mathbf{H}} = \begin{pmatrix} r + \delta \\ r \end{pmatrix} \mathbf{H}, \quad (79c)$$

where

$$\epsilon = \frac{-r\|\mathbf{h}_1\| + g_1}{2N} > 0, \quad (80)$$

$$\delta = \frac{\epsilon}{\max\{\|\mathbf{h}_1\|, \dots, \|\mathbf{h}_{N-1}\|, \|\mathbf{H}\mathbf{1}\|\}} > 0. \quad (81)$$

The polyhedron $\mathcal{P}(\tilde{\mathbf{g}}, \tilde{\mathbf{H}})$ is also an $(N-1)$ -dimensional simplex; this is shown by Fact 3.(b) and the fact that the rank of $\tilde{\mathbf{H}}$ is the same as that of \mathbf{H} (which is full). Now, we claim that $\mathcal{B}(r) \subseteq \mathcal{P}(\tilde{\mathbf{g}}, \tilde{\mathbf{H}})$ and $\text{vol}(\mathcal{P}(\tilde{\mathbf{g}}, \tilde{\mathbf{H}})) < \text{vol}(\mathcal{P}(\mathbf{g}, \mathbf{H})) = \text{vol}(\mathcal{W})$. For the first claim, one can verify from (78)-(79) that

$$-r\|\tilde{\mathbf{h}}_1\| + \tilde{g}_1 \geq (N-1)\epsilon \geq 0,$$

$$-r\|\tilde{\mathbf{h}}_i\| + \tilde{g}_i \geq 0, \quad i = 2, \dots, N-1,$$

$$-r\|\tilde{\mathbf{H}}\mathbf{1}\| + (1 - \mathbf{1}^T \tilde{\mathbf{g}}) \geq \epsilon \geq 0,$$

where $\tilde{\mathbf{h}}_i$ and \tilde{g}_i denote the i th column of $\tilde{\mathbf{H}}$ and i th element of $\tilde{\mathbf{g}}$, resp. The above equations, together with Fact 4.(a), implies that $\mathcal{B}(r) \subseteq \mathcal{P}(\tilde{\mathbf{g}}, \tilde{\mathbf{H}})$. The second claim follows from (68) in Fact 3.(b) and (79c):

$$\begin{aligned} \text{vol}(\mathcal{P}(\tilde{\mathbf{g}}, \tilde{\mathbf{H}})) &= \frac{1}{(N-1)!} \left(\frac{r}{r+\delta} \right)^{N-1} |\det(\mathbf{H})|^{-1} \\ &< \frac{1}{(N-1)!} |\det(\mathbf{H})|^{-1} = \text{vol}(\mathcal{W}), \end{aligned} \quad (82)$$

for $N \geq 2$ (note that $N = 1$ is meaningless). The above two claims contradict the assumption that \mathcal{W} is an MVES of $\mathcal{B}(r)$.

Case 2: Suppose that $\mathbf{t}_N \notin \text{bd}\mathcal{B}(r) \cap \text{bd}\mathcal{W}$. The proof is similar to that of Case 1. Very concisely, this case has $-r\|\mathbf{H}\mathbf{1}\| + (1 - \mathbf{1}^T \mathbf{g}) > 0$ and $-r\|\mathbf{h}_i\| + g_i \geq 0$ for all $i \in \{1, \dots, N-1\}$. By constructing a polyhedron $\mathcal{P}(\tilde{\mathbf{g}}, \tilde{\mathbf{H}})$ where

$$\begin{aligned} \tilde{\mathbf{g}} &= \mathbf{g} + \epsilon \mathbf{1}, \quad \tilde{\mathbf{H}} = \left(\frac{r + \delta}{r} \right) \mathbf{H}, \\ \epsilon &= \frac{-r\|\mathbf{H}\mathbf{1}\| + (1 - \mathbf{1}^T \mathbf{g})}{2N}, \end{aligned}$$

and δ is the same as (81), we show that $\mathcal{B}(r) \subseteq \mathcal{P}(\tilde{\mathbf{g}}, \tilde{\mathbf{H}})$ and $\text{vol}(\mathcal{P}(\tilde{\mathbf{g}}, \tilde{\mathbf{H}})) < \text{vol}(\mathcal{W})$. The above two claims contradict the MVES assumption with \mathcal{W} .

The above two cases imply that $\text{bd}\mathcal{B}(r) \cap \text{bd}\mathcal{W} = \{\mathbf{t}_1, \dots, \mathbf{t}_N\}$, the desired result. In addition to this, Property (a) in Lemma 7 is obvious since the expression of \mathbf{t}_i 's in (70), as well as (67), already suggest the affine independence of $\mathbf{t}_1, \dots, \mathbf{t}_N$. As for Property (b) in Lemma 7, note that (71) are all satisfied. It can be verified that by substituting (70) and (71) into (66), \mathcal{W} can be rewritten as $\mathcal{W} = \bigcap_{i=1}^N \{\boldsymbol{\theta} \in \mathbb{R}^{N-1} \mid r^2 \geq \mathbf{t}_i^T \boldsymbol{\theta}\}$.

E. Proof of Lemma 5

For notational convenience, denote

$$\mathcal{U}(\alpha) = \{\mathbf{s} \in \mathcal{T}_e \mid s_i \leq \alpha, i = 1, \dots, N\},$$

and recall that the aim is to prove $\text{conv}\mathcal{P} = \mathcal{U}(\alpha)$. The above identity is trivial for the case of $\alpha = 1$, since we have $\text{conv}\mathcal{P} = \mathcal{T}_e \equiv \mathcal{U}(1)$ for $\alpha = 1$. Hence, we focus on $0.5 < \alpha < 1$. The proof is split into three steps.

Step 1: We start with showing that $\mathbf{s} \in \text{conv}\mathcal{P} \implies \mathbf{s} \in \mathcal{U}(\alpha)$. Note that any $\mathbf{s} \in \text{conv}\mathcal{P}$ can be written as

$$\mathbf{s} = \sum_{j \neq i} \theta_{ji} \mathbf{p}_{ij},$$

for some $\{\theta_{ji}\}$ satisfying $\sum_{j \neq i} \theta_{ji} = 1$ and $\theta_{ji} \geq 0$ for all $j, i, j \neq i$. From the above equation and the expression of \mathbf{p}_{ij} in (42), one can verify that $\mathbf{s} \in \mathcal{T}_e$, and that $s_k \leq \max_{j \neq i} [\mathbf{p}_{ij}]_k \leq \alpha$ for any k (here $[\mathbf{p}_{ij}]_k$ denotes the k th element of \mathbf{p}_{ij}). Thus, any $\mathbf{s} \in \text{conv}\mathcal{P}$ also lies in $\mathcal{U}(\alpha)$.

Step 2: We turn our attention to proving $\mathbf{s} \in \mathcal{U}(\alpha) \implies \mathbf{s} \in \text{conv}\mathcal{P}$. To proceed, suppose that $\mathbf{s} \in \mathcal{U}(\alpha)$, and assume $s_1 \geq s_2 \geq \dots \geq s_N$ w.l.o.g. From a given \mathbf{s} , choose an index k by the following way

$$k = \max\{i \in \{1, \dots, N\} \mid s_i \geq \delta_i\}, \quad (83)$$

where $\delta_1 = 0$, and

$$\delta_i = \frac{1 - \alpha - \sum_{j=i+1}^N s_j}{i-1}, \quad i = 2, \dots, N. \quad (84)$$

From (83)-(84), the following properties can be shown.

i) It holds true that

$$\begin{aligned} s_1 &\geq \delta_k, \\ &\vdots \\ s_k &\geq \delta_k, \\ s_{k+1} &< \delta_{k+1}, \\ &\vdots \\ s_N &< \delta_N. \end{aligned} \quad (85)$$

- ii) Suppose that $2 \leq k \leq N-1$, and $N \geq 3$. Then \mathbf{s} satisfies $\sum_{j=k+1}^N s_j < 1 - \alpha$.
 iii) For any $\mathbf{s} \in \mathcal{U}(\alpha)$, the index k must satisfy $k \geq 2$.
 iv) $\alpha - \delta_k > 0$ for any $0.5 < \alpha \leq 1$.

The proofs of the above properties are as follows. Property i) follows directly from the definition of k and the ordering of \mathbf{s} . Property ii) is obtained by induction. Observe that if $k \leq N-1$, the last equation of (85) reads

$$s_N < \delta_N = \frac{1 - \alpha}{N-1} \leq 1 - \alpha, \quad (86)$$

and for $k = N-1$ the proof is complete (trivially). For $k < N-1$, we wish to show from (86) that $s_{N-1} + s_N < 1 - \alpha$, and then recursively, $\sum_{j=i}^N s_j < 1 - \alpha$ from $i = N-2$ to $i = k+1$. To put this induction into context, suppose that

$$\sum_{j=i+1}^N s_j < 1 - \alpha \quad (87)$$

for $i \in \{k+1, \dots, N-1\}$, and note that (87) already holds for $i = N-1$ due to (86). The task is to prove $\sum_{j=i}^N s_j < 1 - \alpha$. The proof is as follows:

$$\sum_{j=i}^N s_j < \delta_i + \sum_{j=i+1}^N s_j \quad (88a)$$

$$= \frac{1 - \alpha}{i-1} + \left(1 - \frac{1}{i-1}\right) \sum_{j=i+1}^N s_j \quad (88b)$$

$$< 1 - \alpha, \quad (88c)$$

where (88a) is obtained by $s_i < \delta_i$ in Property i); (88b) by (84); (88c) by (87), and $i-1 \geq k > 1$ for $k \geq 2$. Hence, we conclude by induction that Property ii) holds. To prove Property iii), note that \mathbf{s} satisfies $\mathbf{1}^T \mathbf{s} = 1$. Thus, s_2 can be written as

$$s_2 = 1 - s_1 - \sum_{j=3}^N s_j$$

Since every $\mathbf{s} \in \mathcal{U}(\alpha)$ satisfies $s_i \leq \alpha$ for any i , we get

$$s_2 \geq 1 - \alpha - \sum_{j=3}^N s_j = \delta_2.$$

The above condition implies that $k \geq 2$ must hold. To prove Property iv), observe the following inequalities

$$\alpha - \delta_k \geq \alpha - \frac{1 - \alpha}{k-1} \geq \frac{2\alpha - 1}{k-1};$$

here, the first inequality is done by applying (84), and the second inequality by $k \geq 2$. From the above equation, we see that $\alpha - \delta_k > 0$ for $\alpha > 0.5$.

With the above properties, we are ready to show that $\mathbf{s} \in \mathcal{U}(\alpha)$ lies in $\text{conv}\mathcal{P}$. First, for each $i \in \{1, \dots, k\}$, we construct a vector

$$\bar{\mathbf{p}}_i = \sum_{j \neq i} \theta_{ji} \mathbf{p}_{ij},$$

where

$$\theta_{ji} = \begin{cases} c, & 1 \leq j \leq k, j \neq i \\ \frac{s_j}{1-\alpha}, & k+1 \leq j \leq N, N \geq 3, \end{cases}$$

$$c = \frac{1}{k-1} \left(1 - \frac{\sum_{j=k+1}^N s_j}{1-\alpha} \right) = \frac{\delta_k}{1-\alpha}.$$

It can be verified that $\theta_{ji} \geq 0$, $\sum_{j \neq i} \theta_{ji} = 1$ (in particular, Property ii) is required to verify $c > 0$); that is to say, every $\bar{\mathbf{p}}_i$ satisfies $\bar{\mathbf{p}}_i \in \text{conv}\mathcal{P}$. Moreover, from the above equations, $\bar{\mathbf{p}}_i$ is shown to take the structure

$$\bar{\mathbf{p}}_i = \begin{bmatrix} (\alpha - \delta_k) \mathbf{e}_i + \delta_k \mathbf{1} \\ \mathbf{s}_{k+1:N} \end{bmatrix}, \quad (89)$$

where $\mathbf{s}_{k+1:N} = [s_{k+1}, \dots, s_N]^T$. Now, we claim that

$$\mathbf{s} = \sum_{i=1}^k \beta_i \bar{\mathbf{p}}_i, \quad (90)$$

where

$$\beta_i = \frac{s_i - \delta_k}{\alpha - \delta_k}, \quad i = 1, \dots, k, \quad (91)$$

and they satisfy $\sum_{i=1}^k \beta_i = 1$, $\beta_i \geq 0$ for all i . The above claim is verified as follows. The property $\beta_i \geq 0$ directly follows from Properties i) and iv). For the property $\sum_{i=1}^k \beta_i = 1$, observe that

$$\begin{aligned} \sum_{i=1}^k \beta_i &= \frac{\sum_{i=1}^k s_i - k\delta_k}{\alpha - \delta_k} \\ &= \frac{1 - \sum_{j=k+1}^N s_j - k\delta_k}{\alpha - \delta_k} \\ &= \frac{(k-1)\delta_k + \alpha - k\delta_k}{\alpha - \delta_k} = 1, \end{aligned}$$

where the second equality is by $\mathbf{1}^T \mathbf{s} = 1$, and the third equality by (84). In addition, by substituting (89) and (91) into the right-hand side of (90), and by using $\mathbf{1}^T \mathbf{s} = 1$, one can show that (90) is true. Eq. (90) and the associated properties with β_i suggest that $\mathbf{s} \in \text{conv}\{\bar{\mathbf{p}}_1, \dots, \bar{\mathbf{p}}_k\}$. This, together with the fact that $\bar{\mathbf{p}}_i \in \text{conv}\mathcal{P}$, implies $\mathbf{s} \in \text{conv}\mathcal{P}$.

Step 3: By combining the results in Step 1 and Step 2, we get $\mathbf{s} \in \text{conv}\mathcal{P} \iff \mathbf{s} \in \mathcal{U}(\alpha)$. Lemma 5 is therefore proven.

F. Proof of Lemma 6

Recall $\mathcal{R}(r) = \{\mathbf{s} \in \mathcal{T}_e \mid \|\mathbf{s}\| \leq r\}$, and notice that \mathcal{T}_e can be rewritten as

$$\mathcal{T}_e = \{\mathbf{s} \in \mathbb{R}^N \mid \mathbf{s} \geq \mathbf{0}, \mathbf{1}^T \mathbf{s} = 1\}.$$

Let $\mathbf{s} \in \mathcal{R}(r)$, and assume $s_1 \geq s_2 \geq \dots \geq s_N$ w.l.o.g. From the above assumption, it is easy to verify that $s_1 \geq \frac{1}{N}$. Also, by denoting $\mathbf{s}_{2:N} = [s_2, \dots, s_N]^T$, we have

$$\begin{aligned} r^2 &\geq \|\mathbf{s}\|^2 = s_1^2 + \|\mathbf{s}_{2:N}\|^2 \\ &\geq s_1^2 + \frac{(1-s_1)^2}{N-1} \end{aligned} \quad (92)$$

where the second inequality is owing to the norm inequality $\sum_{i=1}^n |x_i| \leq \sqrt{n} \|\mathbf{x}\|$ for any $\mathbf{x} \in \mathbb{R}^n$, and the fact that $\mathbf{s} \geq \mathbf{0}$, $\mathbf{1}^T \mathbf{s} = 1$. Moreover, equality in (92) holds if \mathbf{s} takes the form $\mathbf{s} = [s_1, \frac{1-s_1}{N-1} \mathbf{1}^T]^T$ (which lies in \mathcal{T}_e). Hence, $\alpha^*(r)$ can be simplified to

$$\alpha^*(r) = \sup s_1 \quad (93a)$$

$$\text{s.t. } s_1^2 + \frac{(1-s_1)^2}{N-1} \leq r^2 \quad (93b)$$

$$\frac{1}{N} \leq s_1 \leq 1. \quad (93c)$$

By the quadratic formula, the constraint in (93b) can be reexpressed as

$$(s_1 - a)(s_1 - b) \leq 0, \quad (94)$$

where

$$\begin{aligned} a &= \frac{1 + \sqrt{(N-1)(Nr^2 - 1)}}{N}, \\ b &= \frac{1 - \sqrt{(N-1)(Nr^2 - 1)}}{N}. \end{aligned}$$

From (93c) and (94), it can be shown that for $\frac{1}{\sqrt{N}} \leq r \leq 1$,

$$b \leq \frac{1}{N} \leq s_1 \leq a \leq 1.$$

Hence, the optimal solution to problem (93) is simply $s_1^* = a$, and the proof is complete.

REFERENCES

- [1] J. M. Bioucas-Dias, A. Plaza, G. Camps-Valls, P. Scheunders, N. Nasrabadi, and J. Chanussot, "Hyperspectral remote sensing data analysis and future challenges," *IEEE Geosci. Remote Sens. Mag.*, vol. 1, no. 2, pp. 6–36, Jun. 2013.
- [2] W.-K. Ma, J. M. Bioucas-Dias, J. Chanussot, and P. Gader, Eds., *Special Issue on Signal and Image Processing in Hyperspectral Remote Sensing*, *IEEE Signal Process. Mag.*, vol. 31, no. 1, Jan. 2014.
- [3] J. Bioucas-Dias, A. Plaza, N. Dobigeon, M. Parente, Q. Du, P. Gader, and J. Chanussot, "Hyperspectral unmixing overview: Geometrical, statistical, and sparse regression-based approaches," *IEEE J. Sel. Topics Appl. Earth Observ.*, vol. 5, no. 2, pp. 354–379, 2012.
- [4] W.-K. Ma, J. M. Bioucas-Dias, T.-H. Chan, N. Gillis, P. Gader, A. J. Plaza, A. Ambikapathi, and C.-Y. Chi, "A signal processing perspective on hyperspectral unmixing," *IEEE Signal Process. Mag.*, vol. 31, no. 1, pp. 67–81, 2014.
- [5] N. Dobigeon, S. Moussaoui, M. Coulon, J.-Y. Tourneret, and A. O. Hero, "Joint Bayesian endmember extraction and linear unmixing for hyperspectral imagery," *IEEE Trans. Signal Process.*, vol. 57, no. 11, pp. 4355–4368, Nov. 2009.
- [6] T.-H. Chan, C.-Y. Chi, Y.-M. Huang, and W.-K. Ma, "A convex analysis based minimum-volume enclosing simplex algorithm for hyperspectral unmixing," *IEEE Trans. Signal Process.*, vol. 57, no. 11, pp. 4418–4432, 2009.
- [7] N. Gillis and S. A. Vavasis, "Fast and robust recursive algorithms for separable nonnegative matrix factorization," *IEEE Trans. Pattern Anal. Mach. Intell.*, vol. 36, no. 4, pp. 698–714, 2014.
- [8] J. Li and J. Bioucas-Dias, "Minimum volume simplex analysis: A fast algorithm to unmix hyperspectral data," in *Proc. IEEE IGARSS*, Aug. 2008.

- [9] M. D. Craig, "Minimum-volume transforms for remotely sensed data," *IEEE Trans. Geosci. Remote Sens.*, vol. 32, no. 3, pp. 542–552, May 1994.
- [10] W. E. Full, R. Ehrlich, and J. E. Klovian, "EXTENDED QMODEL—objective definition of external endmembers in the analysis of mixtures," *Mathematical Geology*, vol. 13, no. 4, pp. 331–344, 1981.
- [11] M. E. Winter, "N-findr: An algorithm for fast autonomous spectral end-member determination in hyperspectral data," in *Proc. SPIE Conf. Imaging Spectrometry*, Pasadena, CA, Oct. 1999, pp. 266–275.
- [12] Q. Du, N. Raksuntorn, N. H. Younan, and R. L. King, "End-member extraction for hyperspectral image analysis," *Applied Optics*, vol. 47, no. 28, pp. F77–F84, 2008.
- [13] T.-H. Chan, W.-K. Ma, A. Ambikapathi, and C.-Y. Chi, "A simplex volume maximization framework for hyperspectral endmember extraction," *IEEE Trans. Geosci. Remote Sens.*, vol. 49, no. 11, pp. 4177–4193, 2011.
- [14] L. Miao and H. Qi, "Endmember extraction from highly mixed data using minimum volume constrained nonnegative matrix factorization," *IEEE Trans. Geosci. Remote Sens.*, vol. 45, no. 3, pp. 765–777, 2007.
- [15] A. Agathos, J. Li, D. Petcu, and A. Plaza, "Multi-GPU implementation of the minimum volume simplex analysis algorithm for hyperspectral unmixing," to appear in *IEEE J. Sel. Topics Appl. Earth Observ.*, 2014.
- [16] J. Bioucas-Dias, "A variable splitting augmented Lagrangian approach to linear spectral unmixing," in *Proc. IEEE WHISPERS*, Aug. 2009.
- [17] A. Ambikapathi, T.-H. Chan, W.-K. Ma, and C.-Y. Chi, "Chance-constrained robust minimum-volume enclosing simplex algorithm for hyperspectral unmixing," *IEEE Trans. Geosci. Remote Sens.*, vol. 49, no. 11, pp. 4194–4209, 2011.
- [18] E. M. Hendrix, I. García, J. Plaza, G. Martín, and A. Plaza, "A new minimum-volume enclosing algorithm for endmember identification and abundance estimation in hyperspectral data," *IEEE Trans. Geosci. Remote Sens.*, vol. 50, no. 7, pp. 2744–2757, 2012.
- [19] M. B. Lopes, J. C. Wolff, J. Bioucas-Dias, and M. Figueiredo, "NIR hyperspectral unmixing based on a minimum volume criterion for fast and accurate chemical characterisation of counterfeit tablets," *Analytical Chemistry*, vol. 82, no. 4, pp. 1462–1469, 2010.
- [20] J. Nascimento and J. Bioucas-Dias, "Hyperspectral unmixing based on mixtures of Dirichlet components," *IEEE Trans. Geosci. Remote Sens.*, vol. 50, no. 3, pp. 863–878, 2012.
- [21] J. Plaza, E. M. Hendrix, I. García, G. Martín, and A. Plaza, "On endmember identification in hyperspectral images without pure pixels: A comparison of algorithms," *Journal of Mathematical Imaging and Vision*, vol. 42, no. 2-3, pp. 163–175, 2012.
- [22] C.-H. Lin, A. Ambikapathi, W.-C. Li, and C.-Y. Chi, "On the endmember identifiability of Craig's criterion for hyperspectral unmixing: A statistical analysis for three-source case," in *Proc. IEEE ICASSP*, May 2013, pp. 2139–2143.
- [23] S. Boyd and L. Vandenberghe, *Convex Optimization*. Cambridge University Press, 2004.
- [24] P. Gritzmann, V. Klee, and D. Larman, "Largest j -simplices in n -polytopes," *Discrete and Computational Geometry*, vol. 13, no. 1, pp. 477–515, 1995.
- [25] A. Packer, "NP-hardness of largest contained and smallest containing simplices for V - and H -polytopes," *Discrete and Computational Geometry*, vol. 28, no. 3, pp. 349–377, 2002.
- [26] P. Gritzmann and V. Klee, "On the complexity of some basic problems in computational convexity: I. containment problems," *Discrete Mathematics*, vol. 136, no. 1, pp. 129–174, 1994.
- [27] T.-H. Chan, W.-K. Ma, C.-Y. Chi, and Y. Wang, "A convex analysis framework for blind separation of non-negative sources," *IEEE Trans. Signal Process.*, vol. 56, no. 10, pp. 5120–5134, 2008.
- [28] R. Clark, G. Swayze, R. Wise, E. Livo, T. Hoefen, R. Kokaly, and S. Sutley, "USGS digital spectral library splib06a: U.S. Geological Survey, Digital Data Series 231," <http://speclab.cr.usgs.gov/spectral.lib06>, 2007.
- [29] L. Gerber, "The orthocentric simplex as an extreme simplex," *Pacific Journal of Mathematics*, vol. 56, no. 1, pp. 97–111, Nov. 1975.



Chia-Hsiang Lin received the B.S. degree in electrical engineering from the National Tsing Hua University (NTHU), Hsinchu, Taiwan, in 2010.

He is pursuing the Ph.D. degree in communications engineering at NTHU. He is currently a visiting Doctoral Graduate Research Assistant of Virginia Polytechnic Institute and State University, Arlington, VA, USA. His research interests are in network science, game theory, convex geometry and optimization, and blind source separation.



Wing-Kin Ma (M'01-SM'11) received the B.Eng. degree in electrical and electronic engineering from the University of Portsmouth, Portsmouth, U.K., in 1995, and the M.Phil. and Ph.D. degrees, both in electronic engineering, from The Chinese University of Hong Kong (CUHK), Hong Kong, in 1997 and 2001, respectively. He is currently an Associate Professor with the Department of Electronic Engineering, CUHK. From 2005 to 2007, he was also an Assistant Professor with the Institute of Communications Engineering, National Tsing Hua University,

Taiwan, R.O.C. Prior to becoming a faculty member, he held various research positions with McMaster University, Canada; CUHK; and the University of Melbourne, Australia. His research interests are in signal processing and communications, with a recent emphasis on optimization, MIMO transceiver designs and interference management, blind signal processing theory, methods and applications, and hyperspectral unmixing in remote sensing.

Dr. Ma is currently serving or has served as Associate Editor and Guest Editor of several journals, which include *IEEE TRANSACTIONS ON SIGNAL PROCESSING*, *IEEE SIGNAL PROCESSING LETTERS*, *SIGNAL PROCESSING*, *IEEE JOURNAL OF SELECTED AREAS IN COMMUNICATIONS* and *IEEE SIGNAL PROCESSING MAGAZINE*. He was a tutorial speaker in *EUSIPCO 2011* and *ICASSP 2014*. He is currently a Member of the Signal Processing Theory and Methods Technical Committee (SPTM-TC) and the Signal Processing for Communications and Networking Technical Committee (SPCOM-TC). Dr. Ma's students have won *ICASSP Best Student Paper Awards* in 2011 and 2014, respectively, and he is co-recipient of a *WHISPERS 2011 Best Paper Award*. He received *Research Excellence Award 2013–2014* by CUHK.



Wei-Chiang Li received the B.S. degree in electrical engineering from the National Tsing Hua University, Hsinchu, Taiwan, in 2009.

Currently, he is pursuing the Ph.D. degree in communications engineering at the National Tsing Hua University, Hsinchu, Taiwan. His research interests are in signal processing problems in wireless communications, and convex optimization methods and its applications.



Chong-Yung Chi (S'83-M'83-SM'89) received the B.S. degree in 1975 and M.S. degree in 1977, from Tatung Institute of Technology and National Taiwan University, all in Electrical Engineering. Then he received Ph.D. degree in Electrical Engineering from the University of Southern California, Los Angeles, California, in 1983.

From 1983 to 1988, he was with the Jet Propulsion Laboratory, Pasadena, California. He has been a Professor with the Department of Electrical Engineering since 1989 and the Institute of Communications Engineering (ICE) since 1999 (also the Chairman of ICE during 2002-2005), National Tsing Hua University, Hsinchu, Taiwan. He has published more than 200 technical papers, including more than 75 journal papers (mostly in IEEE Trans. Signal Processing), 4 book chapters and more than 130 peer-reviewed conference papers, as well as a graduate-level textbook, *Blind Equalization and System Identification*, Springer-Verlag, 2006. His current research interests include signal processing for wireless communications, convex analysis and optimization for blind source separation, biomedical and hyperspectral image analysis.

Dr. Chi is a senior member of IEEE. He has been a Technical Program Committee member for many IEEE sponsored and co-sponsored workshops, symposiums and conferences on signal processing and wireless communications, including Co-organizer and General Co-chairman of 2001 IEEE Workshop on Signal Processing Advances in Wireless Communications (SPAWC), and Co-Chair of Signal Processing for Communications (SPC) Symposium, ChinaCOM 2008 & Lead Co-Chair of SPC Symposium, ChinaCOM 2009. He was an Associate Editor (AE) of IEEE Trans. Signal Processing (5/2001-4/2006), IEEE Trans. Circuits and Systems II (1/2006-12/2007), IEEE Trans. Circuits and Systems I (1/2008-12/2009), AE of IEEE Signal Processing Letters (6/2006-5/2010), and a member of Editorial Board of Elsevier Signal Processing (6/2005-5/2008), and an editor (7/2003-12/2005) as well as a Guest Editor (2006) of EURASIP Journal on Applied Signal Processing. He was a member of Signal Processing Theory and Methods Technical Committee (SPTM-TC) (2005-2010), IEEE Signal Processing Society. Currently, he is a member of Signal Processing for Communications and Networking Technical Committee (SPCOM-TC) and a member of Sensor Array and Multichannel Technical Committee (SAM-TC), IEEE Signal Processing Society, and an AE of IEEE Trans. Signal Processing.



ArulMurugan Ambikapathi (S'02-M'11) received the B.E. degree in electronics and communication engineering from Bharathidasan University, Tiruchirappalli, India, in 2003, the M.E degree in communication systems from Anna University, Chennai, India, in 2005, and the Ph.D. degree from the Institute of Communications Engineering (ICE), National Tsing Hua University (NTHU), Hsinchu, Taiwan, in 2011. He is currently a Senior Algorithm Engineer at Utechzone Co. Ltd., Taipei, Taiwan. He was a Postdoctoral Research Fellow with ICE, NTHU,

from Sep. 2011 to Aug. 2014. His research interests are in hyperspectral and biomedical image analysis, convex analysis and optimization for blind source separation, with recent emphasis on automated object identification and computer vision applications.

Dr. Ambikapathi was the recipient of Gold and Silver medals for academic excellence in his B.E and M.E programs, respectively. He was also the recipient of the NTHU Outstanding Student Scholarship award for two consecutive years (2009 and 2010). He was awarded "The Best Ph.D Thesis Award" from IEEE GeoScience and Remote Sensing Society, Taipei Chapter.